

Nanotube–Polymer Composites for Ultrafast Photonics

By Tawfique Hasan, Zhipei Sun, Fengqiu Wang, Francesco Bonaccorso, Ping Heng Tan, Aleksey G. Rozhin, and Andrea C. Ferrari*

Polymer composites are one of the most attractive near-term means to exploit the unique properties of carbon nanotubes and graphene. This is particularly true for composites aimed at electronics and photonics, where a number of promising applications have already been demonstrated. One such example is nanotube-based saturable absorbers. These can be used as all-optical switches, optical amplifier noise suppressors, or mode-lockers to generate ultrashort laser pulses. Here, we review various aspects of fabrication, characterization, device implementation and operation of nanotube-polymer composites to be used in photonic applications. We also summarize recent results on graphene-based saturable absorbers for ultrafast lasers.

1. Introduction

Fundamental science plays a crucial role in underpinning and generating future technologies. The ability to manipulate the structure and composition at the nanoscale opens new horizons and huge opportunities to create novel materials with superior performance. The introduction of a wide range of new functional materials encompassing polymers, advanced liquid crystals, and nanostructures, including carbon nanotubes (CNTs), nanowires (NWs), and graphene, will have disruptive impact on a variety of devices based on conventional inorganic semiconductors, not only because of cost/performance advantages, but also because they can be manufactured in more flexible ways, suitable for a growing range of applications.

The demand in optical networking for photonic components that meet performance criteria as well as economic requirements opens the door to novel technologies capable of high-yield, low-cost manufacturing, while delivering high performance and enabling unique functions.^[1–3] An optical communication system requires light sources and detectors, but many additional components make up modern transmission networks. Until the end of the 1980s, these, including beam splitters, multiplexers, and switches, consisted of bulk optics, such as lenses and prisms.

These, however, are inconvenient to handle, highly sensitive to misalignment, and prone to instability. All of these problems are avoided in integrated optics systems,^[2,4] which combine miniaturised optical components and waveguides in a highly condensed chip-based device. Their compact, planar layout has advantages over bulk optics, as they permit the reduction of complex multifunction photonic circuits on a planar substrate.

Polymeric materials are the ideal choice for such an integration platform.^[1,5,6] They are easily manipulated by methods such as embossing, stamping, sawing, and wet or

dry etching. They generally have a low-cost room-temperature fabrication process. Polymers can be synthesized with customer-defined optical characteristics such as selective transparency bands in different spectral ranges, variable refractive indexes, low birefringence, etc. Photonic polymers (polyimides, acrylates, silicones) have excellent thermal properties (high thermo-optics coefficient) and good environmental and radiation stability.^[1,2,4,7–9] Siloxane polymers have many attributes that render them viable materials for polymer waveguides.^[1] These can be spin-coated from uncured precursors or polymer solutions and then patterned into the specific waveguide geometries using either reactive ion etch or direct exposure to UV light patterns.^[1] Precise control of the refractive index of both the core and the cladding material can optimise light transmission. Like inorganic materials,^[10] polymers can be doped to take advantage of useful optical properties associated with the dopant.

Optical amplifiers are an important component in optical communications.^[11] They are needed to enhance the signal, particularly in order to compensate for the intrinsic losses due to fiber propagation and splitting, switching, and multiplexing operations. Amplifiers can be housed in optical fibers or in integrated optics components. Erbium-doped fiber amplifiers (EDFAs)^[11] consist of an active region formed from a length of Er-doped silica fiber. They are often used in telecommunication networks to amplify optical signals at around 1550 nm. With the emergence of polymer optical fibers, the natural progression from silica-based EDFAs is the doping of rare earths into polymers.^[12] There has also been increasing interest in doping rare earths in inorganic and organic waveguide components to produce waveguide optical amplifiers.^[13–15] The ease of integrated-circuit fabrication provided by polymers, coupled with the expected high-gain performance in rare-earth materials, lead to increased activity in this field.^[16,17]

[*] Dr. A. C. Ferrari, Dr. T. Hasan, Dr. Z. Sun, Dr. F. Wang, Dr. F. Bonaccorso, Prof. P. H. Tan, Dr. A. G. Rozhin
Department of Engineering
University of Cambridge
9 JJ Thomson Avenue
Cambridge CB3 0FA (UK)
E-mail: acf26@cam.ac.uk
Prof. P. H. Tan
SKLSM
P. O. Box 912, Beijing 100083 (P. R. China)

DOI: 10.1002/adma.200901122

Many of the advantages of polymer materials discussed for communications systems also apply to lab-on-a-chip devices, combining a number of biological and chemical analysis processes into one miniaturized device.^[18] Testing the optical behavior is an important characterization step. Therefore, integrated optics devices are often required in these new systems. The construction of complex lab-on-a-chip devices can be simplified by taking advantage of the ease of fabrication afforded by various polymer-patterning techniques.

Optical gels and adhesives are another class of polymer photonic materials.^[1] They are one of the key components of modern light-wave systems,^[1] and act as light junctions between fiber ends or surfaces of optical devices, filling the gap between two mating parts and minimizing reflections by matching the refractive indexes. Optical gels are silicone-based polymers, with excellent elastic and thermal properties as well as good chemical and environmental stability.^[1,7,19,20] An index-matching gel is obtained by mixing two gels with different refractive indexes in different ratios, in order to get a defined value of refractive index. Most of the gels can then be thermally or UV cured.^[7]

Incorporating nanotubes, nanowires, and graphene derivatives in these materials is a paradigm shift in current technology, creating a new class of photonic polymers not just guiding light, but modulating it, thanks to the functionalities enabled by these nanostructures.

Here, we review the state of the art in fabrication, characterization, incorporation, and operation of nanotube-polymer composites to be used in photonic applications, and, in particular, in ultrashort pulse generation as saturable absorbers. We also summarize recent results on graphene-based saturable absorbers for ultrafast lasers.

2. Nanotubes as Saturable Absorbers

As information-processing approaches the bandwidth-limits of silicon-based devices, new technologies are needed offering the low cost, low power, and high speed necessary for future communication and computing platforms. Standard optical devices are based on traditional semiconductor technology. However, this has hit a limit given by materials and fabrication restrictions. Since transfer rates exceeding 1 Gb s^{-1} strain even the fastest state-of-the-art electronic designs, optical manipulation is suggested as alternative to rapidly transfer information. The backbone of this information technology is composed of optical devices, which allow optical pulses to carry the data that renders information exchanges possible.

Materials with nonlinear optical and electro-optical properties are needed in most photonic applications.^[21–24] Laser sources producing nanosecond to sub-picosecond optical pulses are a major component in the portfolio of leading laser manufacturers. For many scientific, commercial, and industrial uses, solid-state lasers constitute the short-pulse source of choice. They are deployed in a variety of applications ranging from basic scientific research to material processing, from eye surgery to printed circuit-board manufacturing, from metrology to trimming of electronic components, such as resistors and capacitors. Regardless of wavelength, the majority of ultrashort laser systems employ a mode-locking technique, whereby a nonlinear

optical element—called saturable absorber (SA)—turns the laser continuous wave output into a train of ultrashort optical pulses.^[24] The key requirements for nonlinear materials are fast response time, strong nonlinearity, broad wavelength range, low optical loss, high power handling, low power consumption, low cost, and ease of integration into an optical system. The current solutions do not meet all these needs. For example, in present technology, optical switching and modulation is obtained by applying an electric field to crystals such as lithium niobate or to semiconductor heterostructures in order to induce a change in material absorption or refractive index.^[21–24] Each method has its disadvantages. For example, the fabrication of lithium niobate single crystals is complicated, integration into photonic systems is difficult due to the relatively large voltage required, and the environmental stability is poor. Semiconductor heterostructures are expensive to package. They can usually be optimized only for a specific wavelength range, and hence, are not very flexible.

Q-switching and mode-locking are well-established techniques for short-pulse generation.^[21–24] The use of SAs as mode-lockers in solid-state lasers to generate ultrashort pulses was proposed shortly after the invention of the solid-state laser itself.^[25,26] Organic dyes were one of the first materials to be used as SAs.^[27] Color-filter glasses^[28] and dye-doped solids^[29] have also been utilized. Lasers based on these SA materials do not show stable mode-locking because of the short life time of these organic compounds and their low temperature stability.^[24,30–32] At present, the most successful SAs are III–V group binary and ternary semiconductors in the form of multi quantum wells (MQWs).^[31,33–43] These are called semiconductor SA mirrors (SESAMs). Thus far, SESAMs have been widely deployed to mode-lock solid-state lasers in a broad spectral range between 800 and 1550 nm. SESAMs are grown by molecular beam epitaxy (MBE) or metal-organic vapor phase epitaxy (MOVPE) on distributed Bragg reflectors.^[44–48] In addition to strict fabrication requirements, they often undergo high-energy heavy-ion implantation to create defects in order to reduce the recovery time.^[24,45] Also, SESAMs can typically cover a narrow (several tens of nm) operation wavelength range.^[24,31,33,45,49,50] Hence, new materials with strong ultrafast optical nonlinearities, broad operating range, and simple processing and packaging are in great demand.

Solid-state lasers based on thulium or holmium are interesting as they have wide emission from 1.8 to $2.1 \mu\text{m}$.^[51,52] They provide an appropriate tool for high-resolution molecular spectroscopy, atmospheric remote sensing, and medical surgery, as several absorption lines of chemical compounds, such as H_2O , CO_2 , and NO_2 , are present in this range.^[53–56] Tm-doped and Tm–Ho co-doped active media can be pumped by commercially available high-power InGaAs laser diodes at wavelengths around 790 nm, allowing the implementation of efficient, compact, and rugged laser sources.^[53] These devices are particularly important for studies of atmospheric pollution, but no commercial SAs exist for this spectral range at the moment. Due to the wide gain bandwidth of Tm-doped and Tm–Ho co-doped laser systems, sub-100 fs pulse trains at $2 \mu\text{m}$ can be efficiently generated using all-solid-state diode-pumped technology. Short mode-locked pulse trains in this spectral region are of major interest in time-resolved molecular spectroscopy, IR supercontinuum

generation,^[57] and frequency metrology. Moreover, high-energy ultrashort pulses at $\sim 2\ \mu\text{m}$ find specific applications in high-order harmonic and high-efficiency soft-X-ray generation^[58] and for optical relativistic effects.^[59] To date, femtosecond-pulse train generation around $1.9\ \mu\text{m}$ has been demonstrated in passively mode-locked Tm-doped fiber lasers using SESAMs, with pulse durations of $\sim 190\ \text{fs}$.^[60]

The recent advances in nanotechnology have the potential to overcome many of the shortcomings of traditional semiconductor technology. Nanotubes show great promise for optical devices. Single-wall nanotubes (SWNTs) exhibit strong optical absorption, covering a broad spectral range from UV to near IR.^[61–64] To a first approximation, their band gap varies inversely with diameter.^[65] This can, in principle, be fine-tuned by modifying the growth parameters. Isolated semiconducting SWNTs (s-SWNTs) and small SWNT bundles exhibit photoluminescence (PL) in the near-IR spectral range.^[62,66,67] PL is strongly quenched as the bundle size increases, which increases the probability of having metallic SWNTs (m-SWNTs) near s-SWNTs.^[62,67–69] The PL properties of SWNTs have been extensively investigated over the past few years,^[66,67,70–79] and the excitonic nature of electronic transitions in SWNTs has been theoretically predicted^[71,80,81] and experimentally proved.^[70,71] Sub-picosecond carrier relaxation time has also been observed in SWNTs.^[82–86] In addition, they show significant third-order optical nonlinearities, as theoretically predicted^[87–89] and experimentally confirmed.^[86]

The amount of SWNTs needed to assemble a photonic device is very small. At present, the cost of purified SWNTs can be up to $\$1000\text{--}2000/\text{g}$. However, $\sim 4\ \text{mg}$ are enough to prepare a SWNT-polymer composite of $\sim 1600\ \text{mm}^2$ area and $\sim 30\ \mu\text{m}$ thickness, out of which ~ 400 SA devices can be made. Scaled-up production of such devices can further drive costs down. SWNTs also have high laser-damage threshold.^[90–92] In addition, SWNT-polymer SAs can be rendered mechanically robust and environmentally stable with an appropriate choice of host matrix. SAs based on SWNTs thus have great potential to compete with traditional SESAMs.^[93–98] A combination of wet chemistry, organic solvents and polymers with desired optical properties (see Sec. 4.2) has proven an effective route for their fabrication.^[96,99–102]

It is now possible to disperse SWNTs in different solvents.^[103–112] These processed SWNTs can be used in nanotube-polymer composites, opening a viable route for mass production of inexpensive photonic devices and their integration.

Incorporation of tubes into polymers was reported in Ref. [113]. Since then, nanotube-polymer composites developed into a vast research area mostly focused on their mechanical and thermal applications.^[114–118] A notable difference between polymer composites for mechanical applications and optics/ photonics is the method used to incorporate tubes in the host matrix. Strong interaction between tube and polymer is key for mechanical strength. This is typically attained by functionalization^[114,119] and/or in situ polymerization.^[120,121] These methods and the mechanical characterizations of the resultant materials are not covered here. An overview can be found, for example, in Refs. [114,122,123].

For optical-grade composites, fine dispersion without covalent functionalization and control of bundle diameters

are quite useful.^[96,105,124,125] SWNT-polymer composites have thus far been used as electroluminescent^[126,127] and photovoltaic devices.^[126–134] Significant progress was also achieved using percolating SWNT networks and their composites as transparent flexible conductors to replace indium tin oxide (ITO).^[120,135–144]

However, thus far, the most successful photonic/optical applications of SWNT-polymer composites are SAs for mode-locking.^[94–102,125,145–159] Here, SWNTs act as amplitude modulators, absorbing weak optical signals, while letting the strongest pulses pass through without significant loss. Section 3 discusses this in more detail.

The SA composites that are employed for mode-locking can also be used for optical amplifiers noise suppression.^[94] Indeed, optical amplifiers, which exploit stimulated emission of incident light under inverted population conditions, suffer from amplified spontaneous-emission (ASE) noise. Due to this, strong amplification of weak signals becomes a serious issue, especially in long-haul data transmission. This noise can be minimized using SESAMs.^[160] The authors of Ref. [94] realized a similar goal using SWNT SAs.

SWNTs SAs could also be used to fabricate other devices, such as optical switches, modulators, and wavelength converters; preliminary results have been reported.^[161]

Optical limiting is another important nonlinear optical phenomenon, and can be seen as the reverse of saturable absorption. An optical limiting material can strongly attenuate intense, potentially dangerous laser beams, while allowing high transmittance for low-intensity ambient light. This can be utilized to effectively protect delicate optical instruments as well as the human eye. A number of organic materials, including phthalocyanines,^[162,163] porphyrins,^[164] fullerenes,^[165,166] and nanotubes,^[167–171] show strong nonlinear extinction to high-intensity light, hence could serve as candidates for practical optical limiters. Contrary to the saturable absorption effect described above, optical limiting in CNT-based composites is due to nonlinear scattering, originating from heat-induced solvent-vapor bubbles and CNT sublimation. This can cover a broad wavelength range from visible to near IR.^[170] The use of CNT-polymer composites as optical limiters will not be covered here.

3. Saturable Absorption

The response of a material to an electric field can be expressed as:^[172]

$$P = \epsilon_0 \chi E \quad (1)$$

where χ is the dielectric susceptibility, E is the electric field, and ϵ_0 is the permittivity of free space. For very high electric fields, Equation 1 is not sufficient to describe the behavior of some materials. Instead, polarization has to be expressed as a power series in the electric field:^[172]

$$P = \epsilon_0 (\chi_1 E + \chi_2 E^2 + \chi_3 E^3 + \dots) \quad (2)$$

where, χ_1 is the linear susceptibility, while χ_2 and χ_3 are the second- and third-order nonlinear susceptibilities, associated with nonlinear phenomena such as optical parametric oscillation, self-focusing, saturable absorption, two-photon absorption, etc.^[172]

In direct band-gap semiconductors, a variation of the incident light intensity results in changes in absorption and refractive index.^[44] With increasing intensity, the upper energy states fill, blocking further absorption. The material then becomes transparent to photons with energies just above the band edge.^[44] This is known as saturable absorption, and is associated with third-order optical nonlinearities.^[172] The absorption of SAs can be described as^[172–174]

$$\alpha(I) = \frac{\alpha_0}{1 + I/I_{\text{sat}}} + \alpha_{\text{ns}} \quad (3)$$

where I is intensity of the input optical pulse, $\alpha(I)$ is the intensity-dependent absorption coefficient, and α_0 and α_{ns} are the linear limit of saturable absorption and non-saturable absorption, respectively.^[172–174] I_{sat} is the saturation intensity (the intensity necessary to reduce the absorption coefficient to half the initial value, considering $\alpha_{\text{ns}} = 0$).^[172] The dynamic response of the nonlinear absorption is ruled by the recovery time (τ_A), defined as the time necessary to reduce the number of carriers by a factor of $1/e$.^[24] In general, for SAs, a high change in transmission is desired between low and high power irradiation.^[24] For SAs, a low value of α_{ns} is important. This is usually achieved by reducing elastic scattering^[1,175] and other nonsaturable absorption losses arising from polymer matrices and carbonaceous impurities. Most materials demonstrate some saturable absorption, but often only at very high intensities and with relatively low recovery times.^[176]

s-SWNTs are good SAs.^[94–102,125,145–157] Chen et al.^[83] measured saturable absorption in SWNTs at 1550 nm by means of pump-probe spectroscopy, and reported $\chi_3 \sim 10^{-10}$ esu ($1 \text{ esu} = 1.11 \times 10^{-9} \text{ m}^2 \text{ V}^{-2}$). Later, Tatsuura et al.^[84] got $\chi_3 \sim 10^{-7}$ esu in resonant conditions, using a pump pulse with energy equal to that of the eh_{11} transition (where, eh_{ii} is associated with the i -th electronic interband transitions E_{ii} ($i = 1, 2, 3, 4$) in the single particle picture^[66]) in the SWNT absorption spectrum.^[84] This is higher than other nanomaterials and semiconductors.^[177–180] For example, $\chi_3 \sim 10^{-12}$ esu was reported for AgInSe₂ nanorods,^[178] $\sim 10^{-8}$ esu in CdSe,^[181] and $\sim 10^{-12}$ esu in PbS,^[180] which are being investigated, like SWNTs, as alternatives for conventional SESAMs. As a comparison, InGaAs/AlAs/AlAsSb coupled quantum wells prepared in a waveguide structure, used in conventional SESAMs, have $\chi_3 \sim 5.3 \times 10^{-8}$ esu.^[177]

In earlier implementations of SWNTs-SAs, the tubes were directly spray-coated on quartz substrates^[149,182] or used in solution.^[183] Direct synthesis of highly purified SWNT thin films on fiber ends was also proposed.^[184] However, high losses were reported due to residual large aggregates as well as catalyst particles,^[182,184] or the formation of bubbles when SWNTs were used in suspension.^[183] The best way to overcome such disadvantages is to finely disperse SWNTs in a polymer matrix.^[96–102,124,125,146–148,150,152,153,156–159,185–191]

4. Considerations Prior to Preparation of SWNT–Polymer Composites

SWNTs tend to bundle.^[192] Aggregates with dimensions comparable with the device operation wavelength ($\sim 1\text{--}2 \mu\text{m}$) can give rise to significant scattering losses^[193] when used in photonic applications.^[1,98,147,175,194] The first step in the preparation of SWNT–polymer SAs usually involves debundling of the largest aggregates. This is typically achieved using ultrasonication in presence of dispersants (surfactants, polymers, DNA, etc.) in a liquid medium.^[62,63,105,106,195–201] After ultrasonication, the insoluble materials (catalysts, large SWNT bundles) are removed by vacuum filtration or ultracentrifugation. The host polymer, if not used as the dispersant for SWNTs, is then dissolved in the supernatant. Sodium carboxymethylcellulose (NaCMC) is an example of polymer that can be used both as a SWNT dispersant and as host matrix.^[201] Finally, the solvent is gradually evaporated, leaving the tubes incorporated in the matrix. From the application perspective, the selection of nanotubes and host polymer is of great importance. From the fabrication point of view, however, the most critical step is SWNT dispersion and stabilization in an appropriate solvent, without compromising their electronic properties.

4.1. Selection of SWNTs

Selection of nanotubes is very important for the optimum performance of SWNT-based SAs. The nonlinear optical absorption depends on the number of tubes in resonance with the incident light. As the transition energies of SWNTs inversely vary with diameter,^[65] saturable absorption at a particular wavelength depends on the SWNT-diameter distribution.^[202] However, even for an incident wavelength detuned by up to ~ 200 nm from the peak resonance, appreciable saturable absorption can be observed,^[202] probably due to Pauli blocking. In such conditions, higher laser intensity is needed,^[202] which can have detrimental effects to the device performance. Another option is to increase the SWNT loading to attain the desired level of optical density (absorption). This may, however, lead to higher scattering losses from residual catalyst particles and amorphous carbons. Therefore, it is important to match the SWNT absorption to the device operation wavelength.^[96–98,148] Figure 1 shows representative absorption spectra of SWNTs prepared with various growth methods.^[203–205] Due to different diameter distributions, the absorption profiles change. In this particular example, the SWNTs grown by laser ablation, with a diameter range 1.0–1.3 nm,^[147] have a broad peak at ~ 1567 nm, making them the most suitable for the telecommunications C band (1530–1565 nm). The SWNT-diameter distribution can usually be controlled by varying the growth parameters.^[147,204,206] Note that arc discharge and HiPco^[205] samples shown in Figure 1 may also be used, as they have appreciable absorption in the 1550 nm range,^[99–101] but would require increased laser intensity. These SWNTs may be used for mode-locking more effectively at other wavelengths matching their absorption profile. Thus, tuning the SWNT mean diameter is useful for achieving mode-locking at the desired wavelength. Indeed, mode-locking from SWNTs

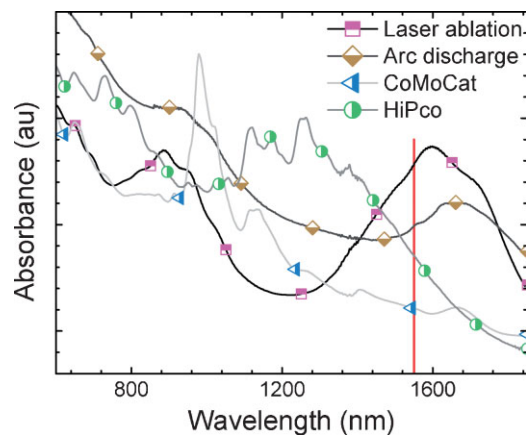


Figure 1. Absorption spectra of SWNTs grown by different methods, with varying absorption profiles. The SWNTs are dispersed in D_2O with SDBS as a surfactant. The vertical line denotes the telecommunications C band (1550 nm).

produced by catalytic CO disproportionation was recently demonstrated in 1.99 μm thalium fiber lasers.^[207]

4.2. Selection of Host Polymers

After the selection of SWNTs, host polymers with desirable optical properties need be chosen. Dispersions are then prepared in solvents in which the target host-polymer matrices can be dissolved and processed. The most desirable characteristics of the host polymer matrices are stability against humidity or other environmental factors and laser irradiation. Long-term thermal stability is another important requirement, as most polymers tend to lose transparency over time due to expulsion of H-halogen molecules and oxidation.^[1] Totally halogenated materials are thus the most stable due to the absence of hydrogen.^[1]

The polymers must also have low absorption losses at the operation wavelength. In polymers, optical absorption in the 1300–1600 nm range is dominated by overtones of fundamental molecular vibrations.^[1,208] The highest energy vibrations arise from the systems with high spring constants; with stiff bonds and/or small reduced masses.^[1,208] The smallest reduced mass occurs when one of the atoms is hydrogen.^[1] Both the C–H and O–H bonds are strongly absorptive in the ~ 1300 – 1700 nm range, while C–F causes the least absorption.^[1] The latter exhibits extremely low absorption through the communication wavelength range, as the absorption due to the C–F bonds in the ~ 1100 – 1600 nm range comes from the 5th, 6th, and 7th overtones of the associated fundamental molecular vibration.^[1,209]

Polymers traditionally employed for broadband communications include polymethylmethacrylate (PMMA), polycarbonate (PC), polystyrene (PS), and epoxy resins.^[1] However, these matrices give a significant optical loss (>0.5 db cm^{-1} , i.e., 89.1% transmission cm^{-1}) at telecommunication wavelengths.^[1,210–212] Several new polymers, mostly deuterated or halogenated polyacrylates and fluorinated polyimides, have been developed

with low loss in the 1000–2000 nm range and good environmental stability.^[209,213–218] Fluorinated polymers are the most transparent for telecommunication applications.^[213,216,218] Introduction of fluorine atoms into hyperbranched polymers improves their thermal and chemical stability, compared to their hydrocarbon counterparts.^[209] Resistance to humidity also improves, resulting in smaller losses from absorbed moisture.^[1,209,215] However, their cost is higher than more traditional materials, such as PMMA or epoxy resins.

Achieving uniform SWNT dispersion in polymer matrices is not trivial. This depends on debundling and resultant bundle diameters. This, in turn, depends on the interaction of the solvent/dispersant molecules with the tube sidewalls. The host polymers are usually mixed after the nanotube-dispersion process. In case of UV-curable polymers with high viscosity, where nanotubes are directly dispersed in polymers without solvent, the effectiveness of ultrasonic systems sharply drops, as high viscosity inhibits bubble formation and collapse.^[219,220] Since ultrasonic-assisted dispersion depends on the shear forces generated by the collapsing bubbles,^[219–222] direct dispersion of isolated SWNTs or sub-micrometer-size bundles using ultrasonic tips is not straightforward. The authors of Ref. [123] reviewed SWNT dispersion in liquid polymers. SWNTs directly dispersed in these are not usually suitable for optical-quality composites, due to the presence of aggregates with micrometer dimensions. Dispersibility of pristine (purified) SWNT hence strongly defines the suitability of polymer matrices. A compromise between optical properties and dispersion compatibility is therefore needed.

In spite of poor environmental stability, water-soluble polymers, such as polyvinylalcohol (PVA), and cellulose derivatives, such as NaCMC, have been widely used for SAs,^[94,97,124,125,147,148,150,153,186,190,194] since stable, high-concentration aqueous dispersions of pristine SWNTs can be easily prepared. From the fabrication perspective, NaCMC is more attractive, as the polymer acts both as a dispersant and host polymer. On the other hand, even though SWNT-PVA first requires the tubes to be dispersed in a water-surfactant solution, it results in mechanically stronger composites and smoother surfaces. Thus, SWNT-PVA composites have been used in studies of saturable absorption and in devices.^[94,97,124,125,147,148,186,194] Polyimides,^[124,150] PC,^[96,100] PMMA,^[99] and styrene methyl methacrylate (SMMA)^[223] have been suggested as alternatives due to their better transparency and environmental stability compared to PVA and NaCMC.

5. Dispersion of Nanotubes in Solvents

In composites for mechanical reinforcement or electrical conductivity, high loading/concentration of de-bundled SWNTs is often desired.^[114,122,123] This can be accomplished by covalent functionalization,^[119,224] which requires defect sites on the SWNT sidewalls for the different functional groups to be attached. This improves de-bundling of SWNTs and their stability in liquid dispersions, especially in organic solvents.^[119,224] For example, fluorinated SWNTs can be dispersed in alcohols.^[119,225] The fluorine atoms can be replaced with alkyl groups, either by treatment with alkyl lithium or with Grignard (alkyl- or

aryl-magnesium halides) compounds.^[226] The treated SWNTs can then be easily dispersed in various organic solvents.^[226] SWNTs reduced with Li or Na can spontaneously disperse, without ultrasonic treatment, in polar aprotic solvents (dimethyl sulfoxide (DMSO), *N,N*-dimethylacetamide (DMA), *N*-methylformamide (NMF), *N*-Methyl-2-pyrrolidone (NMP), dimethylformamide (DMF), etc.).^[120,121] Although covalent functionalization reduces the mechanical strength of SWNTs, it improves the interaction between sidewalls and polymers, resulting in good interfacial stress transfer.^[227] Functionalization also results in better dispersion. This causes a more uniform stress distribution.^[114,119,122,123,224] However, SWNTs can tolerate only a limited number of covalently functionalized sites before their electronic/optical properties significantly change.^[225,228–230] For example, the authors of Ref. [225] reported loss of absorption features for SWNTs functionalized with aryl diazonium salts. The authors of Ref. [230] also observed similar effects by selective covalent functionalization of m-SWNTs by diazonium reagents. For photonic applications, preserving the absorption features is critical. Therefore, covalent functionalization is not the preferred option.

In order to achieve uniform dispersion of SWNTs in polymer composites, *in situ* polymerization under sonication^[120] and *in situ* bulk polymerization^[121] have also been used. The authors of Ref. [120] exploited aromatic polyimides to prepare composites by *in situ* polymerization of the monomers in presence of sonication. *In situ* bulk polymerization was employed by the authors of Ref. [121] to prepare SWNT-PMMA composites from methyl methacrylate (MMA) monomers in presence of the free-radical initiator 2,2-azobisisobutyronitrile (AIBN). Though these approaches improve conductivity and elastic modulus of the composites with low SWNT loading (~0.1 wt%), respectively, the homogeneity of the SWNT dispersion in the composites were not discussed.

Another approach is to use noncovalent interactions, i.e., physical adsorption of solvent or dispersants (surfactants, polymers, biomolecules, etc.) on the SWNT sidewalls.^[62,63,106,201,231–234] This gives little or no change in electronic properties.^[235] A number of polymers have recently been used to disperse SWNTs in non-aqueous media.^[105,107,236–240] These tend to wrap around the tubes or adsorb on the sidewalls, facilitating debundling and stabilization at concentrations appropriate for optical applications (<0.01 wt%).^[105,107,198,223] The difficulty in noncovalent dispersions in non-aqueous solvents is to achieve the desired loading whilst maintaining the resultant dispersion stability.^[105,197,198]

The concentration or loading of SWNTs is an important prerequisite for optical applications, as it offers flexibility in obtaining the desired optical density (absolute absorption). Small bundles containing m-SWNTs are also useful, since m-SWNTs offer a fast relaxation channel for the excited states.

5.1. Dispersion in Water

Pristine SWNTs cannot be stably dispersed in a highly polar solvent like water without functionalization.^[62] Significant effort has been devoted to finding suitable molecules to noncovalently

interact with SWNT sidewalls for the preparation of stable aqueous suspensions. These include surfactants,^[62,106,195,196,241] water-soluble polymers,^[106,195,199,200,241,242] DNA,^[63,64,243,244] polypeptides,^[231–233] and cellulose derivatives.^[201,234,245]

5.1.1. Surfactants

The most commonly used surfactants are sodium dodecyl sulfate (SDS) and sodium dodecyl benzenesulfonate (SDBS).^[62,195,241] Both are linear-chain anionic with a hydrophobic tail and a hydrophilic head.^[195,241] In aqueous solutions, above the critical micelle concentration and at a temperature greater than the critical micelle temperature, the surfactant molecules arrange their hydrophilic heads in contact with water and the hydrophobic tails in the center to form micelles.^[246] The micelles of these surfactants can adopt a wide range of orientations with respect to the tube.^[62] When SWNTs are isolated by the shear forces from the formation and collapse of cavities generated by ultrasounds,^[219,220] surfactants in concentration above the critical micelle concentration form micelles around the individual SWNTs and small bundles, with their nonpolar tail on the SWNT sidewalls, and their polar or ionic end in water. This prevents reaggregation.^[62] Triton X and the Brij series are commonly used among the linear-chain nonionic surfactants.^[106,195] Dodecyltrimethylammonium bromide (DTAB) and cetyltrimethylammonium bromide (CTAB) have also been used.^[106,195] Other anionic surfactants, for example, bile salts, can also disperse SWNTs.^[196,247] Bile salts are flat, rigid molecules, with a hydrophobic and a hydrophilic side.^[248] The most common are sodium cholate (SC), sodium deoxycholate (SDC), and its taurine substitute sodium taurodeoxycholate (TDC).^[106,196,247] In contrast to linear-chain surfactants, the hydrophobic sides of the flat bile-salt molecules adsorb on the sidewalls, resulting in a more regular and uniform coverage around isolated SWNTs.^[196] Pluronic, a series of PEO-PPO-PEO triblock polymers, is also a good dispersant of SWNTs.^[195] Amongst the surfactants, Pluronic F-98 and SDBS disperse the largest amount of SWNTs, but without completely isolating them.^[196]

5.1.2. Polymers

The authors of Ref. [200] first reported the use of reversible, uniform physical adsorption of linear polymers, such as polyvinyl pyrrolidone (PVP) and polystyrene sulfonate (PSS), on to the SWNT sidewalls to get dispersions. PVP also stabilizes surfactant-assisted aqueous SWNT dispersions.^[62] In general, the wrapping of SWNTs by water-soluble polymers is thermodynamically favored by the removal of the hydrophobic interface between SWNT sidewalls and aqueous medium.^[62,199] SWNTs can also be exfoliated in aqueous dispersions of gum arabic (GA), a natural polymer.^[199] GA is a highly branched arabinogalactan polysaccharide with two major components: 70–80% of arabinogalactan, forming a highly branched structure with a hydrodynamic radius (R_h) of ~5 nm, and ~20% of an arabinogalactan-protein complex with a R_h of ~25–50 nm.^[199,249] The authors of Ref. [199] reported that GA adsorbs on SWNT bundles with much smaller dimensions than the characteristic radius (R_F) of the polymeric chains, (25–50 nm in Ref. [199]) and activates a repulsive force at a distance of $2R_F$,^[250] thus helping

the SWNTs to overcome the van der Waals attraction. Linear polysaccharides, such as chitosan, can also disperse SWNTs.^[106,245] The loading is comparable to that of the SBDS and Pluronic series of surfactants.^[106,195]

5.1.3. DNA and other Biomolecules

DNA is a good SWNT dispersant in aqueous environments.^[63,64,243,251–254] The authors of Ref. [63] suggested that single-stranded DNA (ss-DNA) forms a helical wrap around SWNT sidewalls by π -stacking. They showed that the binding free-energy of ss-DNA to SWNTs is higher than that between two SWNTs, thus facilitating dispersion.^[63] Other biomolecules, such as polypeptides, are also efficient for aqueous dispersions.^[231–233] For example, the authors of Ref. [231] designed a peptide, called nano-1, which folds into an α -helix. Its hydrophobic side interacts with the SWNT sidewall, whereas the hydrophilic side interacts with the aqueous medium.^[237] Increasing the number of aromatic residues within the peptides improves the dispersion quality.^[232] This can be further improved by crosslinking the peptides on the external side of the α -helices.^[233] Carboxymethylcellulose^[201,234] and hydroxyethylcellulose^[201] have also been reported to isolate SWNTs with higher loading compared to the surfactants and polymers discussed in Sections 5.1.1 and 5.1.2. Recently, NaCMC was used to prepare optical-quality SWNT-NaCMC SA composites through the aqueous-solvent route.^[153,190]

5.2. Non-Covalent SWNT Dispersions in Non-Aqueous Solvents

For non-aqueous, solvent-based dispersions, loading, stability, and reaggregation of the tubes are major issues. Most humidity-resistant SWNT-polymer composites (with PC, polyimide, PMMA, SMMA, etc.) need to be prepared through the non-aqueous solvent route.

5.2.1. Pure Non-Aqueous Solvents

Dispersion of pristine SWNTs in pure amide solvents, such as DMSO, DMA, NMF, NMP, DMF, etc. is possible, but only at low concentrations.^[104,111,112,197,255,256] The authors of Ref. [111] reported a list of desired solvent properties for SWNT dispersions. Important criteria for solvents to get good dispersion of unfunctionalized SWNTs include high electron-pair donicity (β , i.e., hydrogen bond acceptance ability),^[257,258] small hydrogen-bond donation parameter (α), and high solvatochromatic parameter (π^*).^[111] The latter describes the polarity and polarizability of solvents.^[257,258] Therefore, the Lewis basicity,^[111,257,258] without hydrogen donors, is the key to good dispersion of SWNTs. This is necessary but does not cover all the requirements, since the authors of Ref. [111] also found that DMSO meets all the above criteria but is only a mediocre solvent for SWNTs. In highly polar alkyl amide solvents, bond lengths and angles are important criterions for good SWNT dispersion.^[112] Amongst the amide solvents, NMP is one of the most effective for dispersing pristine SWNTs. Recently, the authors of Ref. [110] reported that interaction between pristine HiPco SWNTs with NMP leads to an almost zero enthalpy of mixing, facilitating SWNT dispersion in pure NMP. Up to $\sim 70\%$ of individual tubes at a very low concentration ($\sim 0.004 \text{ g L}^{-1}$) can be

obtained using this strategy. The average bundle diameter increases with SWNT concentration.^[104] Individual SWNTs remain stable in NMP for at least three weeks.^[197,198] However, such low concentrations do not allow fabrication of composites with the optical density ($\sim 0.2\text{--}0.5$) required for SAs.^[96,125,147]

5.2.2. Non-Aqueous Solvent with Dispersants

For non-aqueous solvents, debundling of SWNTs can be achieved using polymers, which can also limit reaggregation. This is thought to happen by physical adsorption/wrapping by polymers through π -stacking.^[96,105,197,198,236–240,259] The choice of dispersant molecules is, however, not as broad as in the case of aqueous dispersions. Only a handful of organic solvent-dispersant combinations may be used to prepare stable SWNT dispersions with >0.01 to $<0.05 \text{ wt}\%$ loading.^[96,105,107]

We recently reported that PVP can significantly improve the stability and loading ($\sim 0.14 \text{ g L}^{-1}$) of isolated, unfunctionalized SWNTs in NMP.^[105,197,198] PVP debundles reaggregated SWNTs.^[197,198] SWNTs have also been dispersed in low-viscosity MMA, which is then thermally polymerized.^[99] The authors of Ref. [99] reported that addition of diphenyl sulfide and benzyl benzoate reduces reaggregation. Conjugated polymers can also disperse SWNTs in organic solvents. For example, polythiophene derivatives poly[3-(2-methoxyethoxy)ethoxymethylthiophene-2,5-diyl]^[260] and regiorandom poly(3-hexylthiophene) were reported to be efficient dispersant in chloroform.^[107] We used regioregular poly(3-hexylthiophene-2,5-diyl) (P3HT) to disperse and stabilize laser-ablation SWNTs with $\sim 1.3 \text{ nm}$ diameter in 1,2-dichlorobenzene (DCB).^[96] This is quite useful, since SWNTs with such diameters are ideal as SAs at the telecommunication C band.^[96,147]

Amphiphilic block copolymers may also be used to isolate SWNTs in DMF.^[261] They act as surfactants, having hydrophobic and hydrophilic blocks. Polystyrene-*block*-polyacrylic acid (PS-*b*-PAA) forms micelles around SWNTs due to the gradual addition of water. The external hydrophilic blocks can then be crosslinked, creating stable micelles.^[261]

Poly-[(*m*-phenylenevinylene)-*co*-(2,5-dioctyloxy-*p*-phenylenevinylene)] (PmPV) and its derivatives preferentially wrap bundles, rather than individual tubes, when chloroform is used as solvent.^[237,239] PmPV derivatives containing ionic side-groups can also disperse SWNT bundles in protic solvents, such as ethanol.^[240] The dispersion mechanism is proposed to be π -stacking and van der Waals interaction between the PmPV molecules and SWNT sidewalls.^[240] On the other hand, if a hyperbranched variant of PmPV is used, SWNTs can be individually dispersed in chloroform.^[238] In this case, the branched structure of the polymer forms cavities suitable to host individual SWNTs.^[238] Isolated SWNTs can also be obtained in tetrahydrofuran (THF) if poly(*p*-phenylene-1,2-vinylene) (PPV) is copolymerized with units of *p*-phenylene-1,1-vinylidene.^[236] The resulting copolymer (coPPV) has structural defects (the 1,1-vinylidene units) that allow the polymer backbone to fit the curvature of the tube sidewalls better than the homopolymer, thus wrapping the SWNTs by π -stacking.^[236] Amongst the polymers used for SWNT dispersion, PVP and polythiophene derivatives are most suitable due to high loading and ease of dispersion.^[96,105,107]

5.3. Characterization of SWNT Dispersions

SWNT dispersions with low loading (<0.01 wt%) can be characterized by photoluminescence excitation (PLE), optical absorption spectroscopy (OAS), and Raman spectroscopy. These methods are employed to assess concentration and presence of individual SWNTs or small bundles, and may be used as independent or complementary characterization tools.^[62,67,68,103–105,196,197,262,263,266] OAS is mostly used to study the SWNT dispersion. PLE can be employed to study dispersion/aggregation of SWNTs,^[67,68,105,262,263,266] to compare the relative population of different SWNT species,^[196,267] the stability of dispersions,^[67,197,268] etc.

5.3.1. Optical Absorption Spectroscopy

Figure 2 plots absorption spectra of SWNTs dispersed in several solvent-surfactant systems. The peaks are excitonic transitions. For example, the features from 400 to 550 nm, 550 to 900 nm, and 1100 to 1430 nm are eh_{11} of m-SWNTs, eh_{22} of s-SWNTs, and eh_{11} of s-SWNTs, respectively.^[62,269] These can broaden and shift due to change in the dielectric constant (ϵ) of the surrounding environment, as a result of bundling^[67,68,270,271] or different surfactant coverage.^[106,195,196,241] Indeed, up to 10 meV red-shift in the exciton energy was attributed to bundling.^[67,68,270,271] The authors of Ref. [104] reported a red shift from 30 to 50 meV for SWNT dispersions in pure NMP, compared to aqueous SWNT dispersions. A similar shift is seen in Figure 2. Along with the exciton-binding energy, dielectric screening reduces the

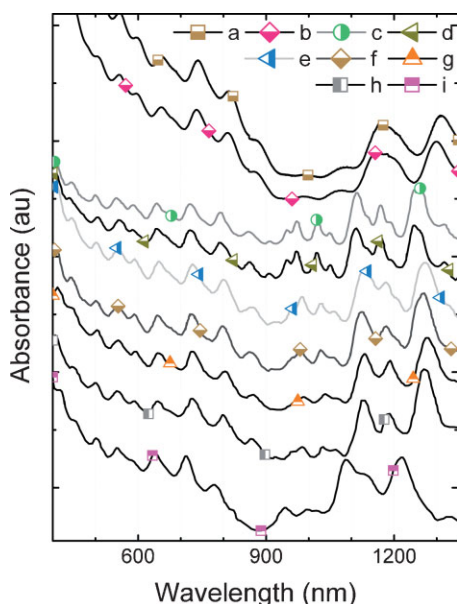


Figure 2. Absorption spectra of HiPco SWNTs in different solvent-surfactant system: a) NMP/PVP [197]; b) Pure NMP [197]; c) Water/SDBS [195]; d) Water/SDS [195]; e) Water/CTAB [195]; f) Water/Brij [195]; g) Water/Na-CMC [201]; h) Water/DNA [63]; i) Water/nano-1 peptide [232]. The spectra illustrate the shift in absorption due to different dielectric environments surrounding the SWNTs. Note the peaks broadening and loss of sharp features in organic solvent dispersions.

electron–electron interaction. This is why the overall shifts are small in spite of large change in the dielectric environment.^[272]

When preparing composites for optical applications, estimation of SWNT aggregation in the dispersions is usually carried out by comparing solutions prepared using the same dispersant/solvent combination, to eliminate the effects caused by different dielectric environments. However, more specific information on SWNT aggregations can be obtained using PLE spectroscopy, which we will briefly discuss in Section 5.3.1.2.

5.3.1.1. Quantitative Estimation of SWNT Concentration

Estimation of SWNT loading enables the determination of the required amount of polymer to achieve the desired optical density in the resulting SWNT–polymer composite. The SWNT concentration can be assessed by the Beer–Lambert law $A_\lambda = \alpha_\lambda lc$, where A_λ is the absorbance at wavelength λ , α_λ is the absorption coefficient at wavelength λ , l is optical path length, and c is the concentration. In case of a very high SWNT concentration, the dispersion needs to be diluted to avoid scattering losses.^[105,112] In order to get a reliable result, it is necessary to determine α_λ at several wavelengths from a set of solutions with known SWNT concentration.^[105,112,197] Figure 3 shows an example used to estimate α_λ of HiPco SWNTs in pure NMP.^[197] The wavelengths are chosen to match peaks in the absorption spectra of HiPco SWNTs in NMP, such as eh_{11} of m-SWNTs (at 506 nm), eh_{22} of s-SWNTs (at 660 and 871 nm), and eh_{11} of s-SWNTs (at 1308 nm). This can then be used to assess the SWNT concentrations of other dispersions in pure NMP.^[105,197]

5.3.1.2. Qualitative Estimation of Bundling

The amount of bundling in both aqueous and organic solvent dispersions is another key parameter. The stability and aggregation of the dispersed SWNTs in solvents determine the bundle size in the composite.^[105] If SWNTs are completely isolated, the relaxation of the excited states is slower compared to that of SWNTs in bundles.^[67] On the other hand, bundles

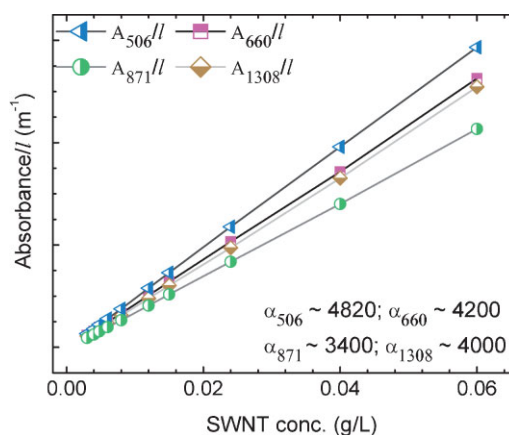


Figure 3. Absorption coefficients of HiPco SWNTs in NMP at four different wavelengths. Adapted from [197].

with size comparable to the operation wavelength cause unwanted scattering losses.^[1,175,193] Therefore, a compromise in bundle diameter must be reached, to minimize losses and recovery time.

PLE may be used to identify bundles by monitoring the optical signatures of exciton energy transfer (EET).^[67,68,268] Detection of EET does not require any reference sample. For example, we observed that, two months after preparation, CoMoCAT^[203] dispersions in water with 1 wt% SDBS form small bundles.^[67] This was suggested by the red-shift in eh_{11} emission wavelengths.^[271,273] However, we also detected a number of new peaks, not corresponding to any previously reported exciton–exciton resonances of SWNTs in the emission range from 1150 to 1350 nm.^[66,274] We attributed these to EET from large-bandgap s-SWNTs (donors) to small-bandgap s-SWNTs (acceptors). Figure 4a and b schematically describe EET from a donor to an acceptor SWNT. Note that these optical features are distinct from the emission satellites of bright phonon sidebands,^[275] since the intensity of those features is only a few percent compared to the main eh_{11} peaks, even for isolated SWNTs.^[268] In bundles, these should become weaker due to the presence of additional excitonic relaxation channels via EET.^[67] Also, the positions of the bright phonon sidebands depend on the associated excitonic-transition energies.^[268] On the other hand, EET band can be very strong and only depend on the transition energies of donor and acceptor s-SWNTs.^[67] EET from (6,5) to (8,4) in as-prepared and two-month-incubated dispersions are shown in Figure 4c and d. Note the change in the relative intensities of the (8,4) exciton–exciton transition, and the associated EET feature indicated by a circle. Figure 4e shows some of the most prominent EET features as circles and ellipses. EET can therefore be used as an equally effective tool to detect the presence of bundles in both aqueous^[67,68,268] and non-aqueous^[105] dispersions.

6. Incorporation of SWNTs into Host Polymers

After ultrasonication, the dispersions in aqueous or non-aqueous media usually contain large insoluble residuals (catalyst particles) and SWNT aggregates/bundles.^[62] These are generally removed by centrifugation or vacuum filtration.^[62] There is always a trade-off between the desired bundle diameter and SWNT loading. In contrast to non-aqueous dispersions, high loading can be easily achieved in aqueous dispersions. After the removal of aggregates, the dispersions are mixed with the host polymer.^[125,147,186] The same protocol is followed in organic solvents if a different polymer is used as the SWNT dispersant.^[96,105,124,223] The mixtures are then drop-cast or spin coated, depending on the application requirements. In general, the thickness requirement for composites sandwiched between fiber connectors is $\sim 10\text{--}30\ \mu\text{m}$ to reduce insertion losses. Even thinner composites are favored for the same reason. However, high SWNT loading is required to obtain the desired level of optical absorption ($\sim 0.2\text{--}0.5$).^[96,125,147] Also, thin films can be fragile. In case of a free-space setup, thicker composites can be used. For example, the authors of Refs. [100,102] prepared SWNT-PS, SWNT-PMMA and SWNT-PC SA composites as thick as 1 mm.

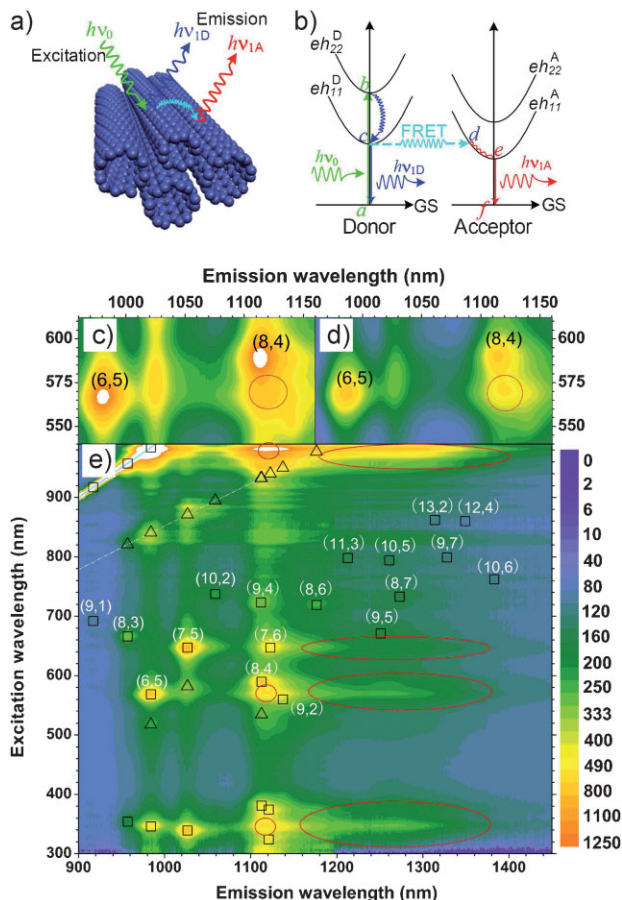


Figure 4. EET from large-gap s-SWNT to a smaller-gap s-SWNT: a) schematic, b) excitonic picture. PLE map for c) as-prepared dispersions and d) after two months. PLE maps show the intensity of emission as a function of excitation wavelength (300–900 nm) and emission wavelength (900–1400 nm). Open squares represent eh_{11} emission of SWNTs matching their eh_{11} , eh_{22} , eh_{33} , and eh_{44} transitions. The (eh_{22}, eh_{11}) resonances are labeled with the chiral index of the corresponding SWNT. Open up-triangles are phonon sidebands of eh_{11} and eh_{22} excitons. Open circles mark emission from (8,4), (7,6), (9,4), with excitation matching eh_{11} , eh_{22} , and eh_{33} of (6,5). Broad spectral features marked by ellipses are assigned to EET between s-SWNTs. Adapted from [67].

6.1. Aqueous-Solvent Route

As mentioned in Section 4.2, the most common water-soluble polymers for SWNT–polymer SAs are PVA and NaCMC.^[94,97,124,125,147,148,150,153,186,190,194] Their optical quality and mode-locking performance has steadily improved.^[97,125,147,148,156,186]

For PVA, SDBS may be used as surfactant due to its efficiency in dispersing high amounts of SWNTs.^[106,195,196] It disperses SWNTs with a larger diameter range compared to bile salts, the latter preferring small-diameter tubes.^[196] The amount of SWNTs and dispersant vary according to the SWNT purity. The duration of sonication depends on the ultrasonicator and sample temperature during the dispersion process. For example, homogeneous dispersions can be achieved by ultrasonating 0.02–0.05 wt% (0.2–0.5 mg mL⁻¹) of purified HiPco SWNTs with 0.2 wt% (2 mg mL⁻¹) of SDBS for 2–3 h at 10–12 °C using a

Bioruptor (Diagenode) sonicator system^[276] operating at 20 kHz with 270 W power. Note that the actual power delivered to the sample is substantially lower due to noncontact dispersion method of this ultrasonicator. Depending on the quality of the ultrasonicated dispersion, ultracentrifugation is carried out at 80 000–140 000g for 1–2 h.^[97,125] The supernatant is then decanted. The maximum eh_{11} absorption usually varies from 1–1.5 (~10–3% transmission)^[125] depending on SWNT diameter distribution and purity. The dispersion is then mixed with 20–30 wt% aqueous PVA solution. Ultrasonication of the mixture results in a uniform solution, which is then drop cast on a Petri dish. Slow evaporation (1–2 weeks) under ambient temperature and pressure results in a free-standing SWNT-PVA composite with homogeneously dispersed tubes.^[94,125,147,148,185,186,194]

SWNT-NaCMC composites require one step less, since NaCMC acts as dispersant as well as host polymer.^[153,190,201,234] Typically, 0.02–0.05 wt% (0.2–0.5 mg mL⁻¹) SWNTs with 1–1.5 wt% (10–15 mg mL⁻¹) Na-CMC are ultrasonicated for 2–3 h at 40–60 °C using a Branson tip sonicator at 20 kHz with 200 W power. The dispersion is then centrifuged at 120 000–150 000g for 1–2 h.^[153,190] The decanted dispersion is then drop-cast under ambient pressure. However, NaCMC is hygroscopic, hence its poor environmental stability.^[277]

6.2. Non-Aqueous-Solvent Route

SWNT polymer composites with polyimide,^[124,150] polystyrene (PS),^[102] PMMA,^[99,102] PC,^[96,100] SMMA,^[223] and P3HT^[101] have thus far been demonstrated as SAs in transmissive device configurations. Compared to PVA and NaCMC, these composites are more environmentally stable.^[1] In addition, they are more transparent in the telecommunications C band region.

The authors of Ref. [124] prepared the first SWNT-polymer composite for optical applications through the non-aqueous-solvent route. They used polyimide as the host matrix. After the ultrasonic-assisted dispersion of purified SWNTs in NMP and subsequent ultracentrifugation, the supernatant was mixed with block-copolymerized polyimide soluble in NMP. The mixture was then coated on glass substrates and cured at 90 °C for 1 h, and then at 180 °C for another hour. The cured polymer composite was then separated from the substrate. No detectable aggregation was observed under optical microscopy in the free-standing composite.^[124] The authors of Ref. [102] prepared PS and PMMA composites using chlorobenzene or tetrahydrofuran (THF). The resulting uniform dispersion of SWNTs by PMMA was assigned to the intermolecular force between a carbonyl group of PMMA and open ends and sidewall defects of SWNTs. The composites were then used as SAs.^[102]

Recently, we prepared SWNT-PC composites by dispersing tubes in DCB using P3HT as the dispersant.^[96] Ultrasonication of 0.05–0.08 wt% (0.5–0.8 mg mL⁻¹) purified SWNTs with 0.4 wt% (4 mg mL⁻¹) P3HT for 3 h at 20 °C using a tip sonicator was used to get a homogeneous dispersion. This was then centrifuged at 300 000g to remove large aggregates. Pellets of PC, a copolymer of bisphenol A and bisphenol TMC, were added and dissolved by further ultrasonication. The resulting SWNT-P3HT-PC dispersion in DCB was drop-cast in a Petri dish under vacuum at room

temperature, producing a free-standing film with uniform, sub-micrometer SWNT aggregation across the composite.^[96] We used a similar SWNT-P3HT dispersion in chloroform mixed with SMMA to produce a homogeneous SWNT-P3HT-SMMA composite.^[223] To minimize aggregation, the composite was dried slowly under saturated chloroform vapor.^[107,223] The authors of Ref. [101] used SWNT-P3HT in chloroform to dip-coat directly on a fiber connector end. A PC composite was also reported in Ref. [100]. SWNTs were mechanically mixed with DMF and then ultrasonicated in presence of PC. Drop-casting resulted in a composite with rough surface, then polished to obtain a mirror-like finish.^[100] However, the power transmission at the device operation wavelength was less than 1%.^[100]

Significant progress has been achieved over the past five years on SWNT-polymer composites prepared via the organic-solvent route. The composites discussed here have long-term environmental stability compared to PVA and NaCMC. In particular, PC has higher heat resistance than most other polymers discussed here.^[1,211] The challenge now is to prepare composites with silicone and hyperbranched fluorinated polymers, to further improve performance and stability of the transmissive-type device structures. Both these classes of polymers offer the unique advantage of high water repellence, heat stability, and extreme resistance to chemical attacks.^[1,209]

6.3. Characterization of Saturable Absorber Composites

6.3.1. Optical Microscopy

In order to optimize the SA performance, it is important to ensure the composite is free from cracks, bubbles, particles, aggregations, and other physical defects that introduce nonsaturable losses. These defects cause losses when their dimensions are comparable to the device-operation wavelength.^[175] Therefore, optical microscopy is an adequate tool.

Figure 5 shows optical microscopy images of PVA, NaCMC, SMMA, and PC composites with SWNTs. No significant aggregation can be resolved. The darker pattern in the SWNT-NaCMC composite is due to higher surface roughness. Note that composites with a significant amount of large aggregates (SWNT bundles, undissolved particles, etc.) can still function as SAs, but with lower performances.

6.3.2. Optical Absorption Spectroscopy

The optical density of SA composites at the device-operation wavelength is an important indicator of the expected performance.^[148] This can be determined by OAS. The generally acceptable range of optical density is 0.2–0.5 (60–30% transmission).^[94,96–98,124,125,147,156,186] However, composites with much higher absorption have also been demonstrated to mode-lock.^[100] As an example, Figure 6a shows the absorption of SWNT-PVA, pure PVA, and the initial SWNT solution.^[125,186] The shift in the SWNT absorbance peaks in the host polymer compared to the solution can be attributed to a change in dielectric environment,^[271,272,278] as well as mechanical stress on the nanotubes.^[279] For a comparison, a similar set of spectra for a SWNT-P3HT-PC composite is presented in Figure 6b.

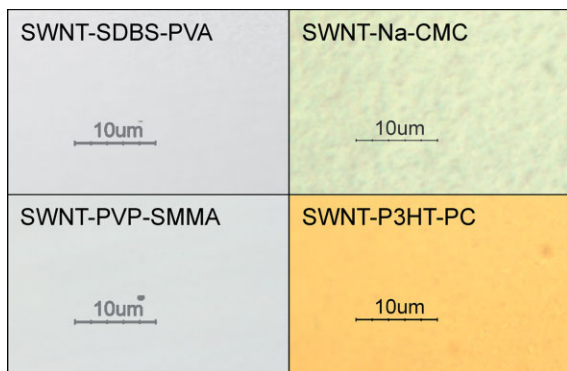


Figure 5. Optical microscopy images of SWNT–polymer composites. The SWNT-SDBS-PVA and SWNT-NaCMC composites are prepared using a similar slow evaporation protocol at ambient temperature and pressure, resulting in higher surface roughness in the latter. The SWNT-PVP-SMMA and SWNT-P3HT-PC composites are prepared using vacuum evaporation. The golden tint in the SWNT-P3HT-PC composite arises from P3HT.

OAS also provides other important insights. Comparison between the SWNT absorbance spectra in D₂O and DCB shows that the narrow SWNT absorption features in D₂O broaden and red-shift in DCB. This indicates larger bundles in the latter dispersion,^[62,273] which is further confirmed by the absence of PL in DCB.^[96] A significant absorbance increase in the region below 1100 nm is observed in the SWNT-P3HT-PC composite. This is

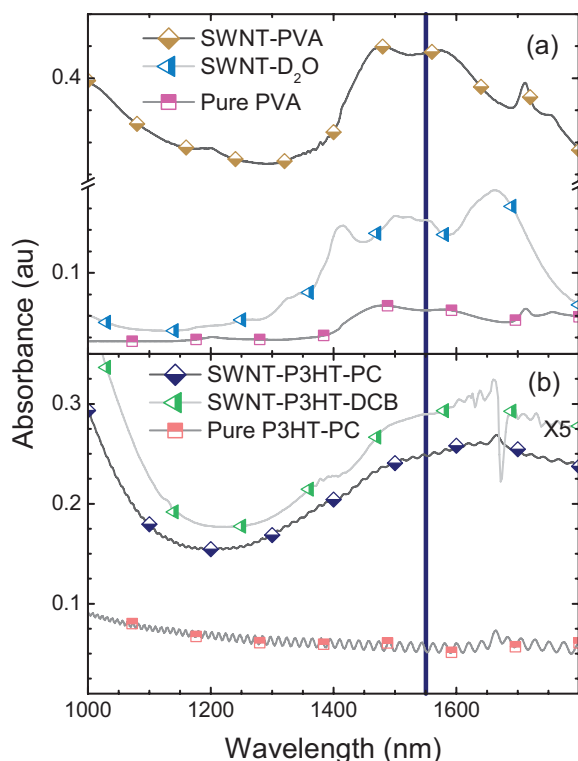


Figure 6. Absorption spectra of laser-ablation SWNT dispersions: a) in D₂O-SDBS and b) in P3HT-DCB; composite in a) PVA, b) P3HT-PC. Adapted from [96]. Absorption from the pure polymers without the nanotubes is also presented. The vertical line denotes the operating wavelength for the telecommunications C band (1550 nm).

most likely due to π – π interactions between P3HT and SWNTs,^[236] as pure P3HT in DCB does not absorb above 600 nm.^[96] Alignment of SWNTs can also be studied using OAS, as the intensity of SWNT absorption peaks decrease with increasing polarization angle.^[194,201,280]

6.3.3. Raman Spectroscopy

Raman spectroscopy can be used to confirm the presence of SWNTs within a composite and their diameter distribution. It may also be used to estimate the ultrasonication or laser-induced damage. As an example, Figure 7 shows Raman spectra of SWNT-PVA composites, as well as the starting SWNTs, taken at 514, 633, and 785 nm excitation.

In the 1500–1600 cm^{−1} region, a typical Raman spectrum of SWNT consists of the G⁺ and G[−] bands. In s-SWNTs, they originate from the longitudinal (LO) and tangential (TO) modes, respectively, derived from the splitting of the E_{2g} phonon of graphene.^[281–284] In m-SWNTs, instead, the assignment of the G⁺ and G[−] bands is the opposite, and the G[−] width is larger.^[281,282] Thus, the presence of a wide, low-frequency G[−] is a fingerprint of m-SWNTs. However, the absence of such feature does not necessarily mean that no m-SWNTs are present, but could just signify that those are off-resonance, or, less likely, that only arm-chair m-SWNTs are present (since in this case the LO mode is forbidden by symmetry). Thus, the use of a large number of excitation wavelengths is necessary for a complete characterization.^[278,285] However, some information can be derived with just two–three wavelengths, especially in the case of process monitoring, such as in composites preparation, when Raman spectroscopy is used to compare the initial material, the resulting solutions and composites, as in Figure 7.

In the low-frequency region, the radial breathing modes (RBMs) are observed.^[286,287] Their energy is inversely related to SWNT diameter, *d*, by the relation: $\omega_{RBM} = \frac{C_1}{d} + C_2$.^[66,278,286–288,290–295] Several groups have derived a variety of C₁ and C₂.^[66,278,286–288,290–295] Combining the information given by the RBMs with the excitation wavelength through the ‘Kataura plot’,^[65,269] it is in

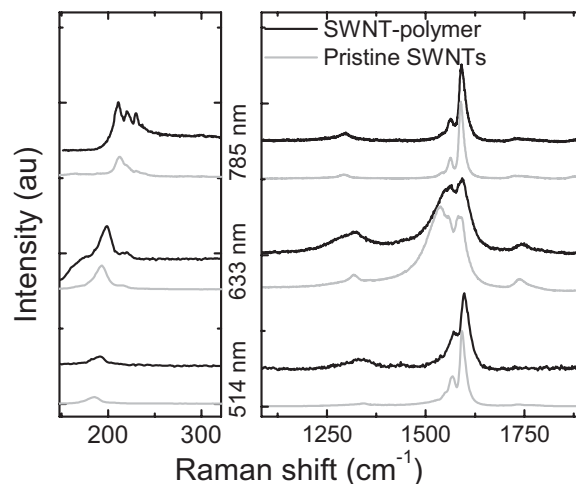


Figure 7. Raman spectra of pristine SWNTs and SWNT–polymer composite. The corresponding excitation wavelengths are also indicated.

principle possible to derive the SWNT chirality.^[292,296,297] Refs. [278,285,288,289] report tables where for each (n,m) , the corresponding RBM and transition energies are assigned.

However, if we are just interested in an estimation of the band gap, any parameter can be used, as the difference in the calculated diameter is negligible. For example, let us consider two well-separated RBM frequencies (100 and 350 cm^{-1}) and calculate the diameter using the two most different values for C_1 (218 and 261) found in Refs. [278,295]. For the higher RBM frequency (smaller diameters) the calculated diameters (0.62 nm and 0.75 nm) differ from their average by $\sim 10\%$. An average bandgap of ~ 1.3 eV can be inferred,^[206] from which the two extremes deviate by $\sim 8\%$. For the lower RBM frequency (larger diameters), the calculated diameters (2.18 nm and 2.61 nm) differ from their average by $\sim 10\%$; an average band gap of ~ 0.35 eV can be inferred, from which the two extremes deviate by $\sim 9\%$. Thus, the evaluation of optical absorption through the Kataura plot^[65] is not deeply affected.

Matching the diameter given by RBM with the excitation wavelength in the Kataura plot gives information on the semiconducting or metallic character. For example, in the spectra shown in Figure 7 at 514 nm, the RBM is 186 cm^{-1} , from which a diameter 1.29 nm is derived. From Ref. [65], we deduce that s-SWNTs are excited. At 633 nm, the RBM is 193 cm^{-1} , from which a diameter 1.23 nm is derived, and from Ref. [65], we deduce that m-SWNTs are excited. Thus, Figure 7 shows that the sample is a mixture of m-SWNTs (at 633 nm) and s-SWNTs (observed at 514 and 785 nm). This is further confirmed by the shape of the G^- band.^[281,298]

Raman spectroscopy can also be used to verify any possible damage during ultrasonic dispersion, as well as laser-induced damage during SA operation, by monitoring the D peak and its overtone, the $2D$ band.^[299–301] In Figure 7, the small increase of the D to G intensity ratio, $I(D)/I(G)$, from the pristine sample to the composite, indicates that the dispersion causes limited damage. Figure 8 compares the Raman spectra of the

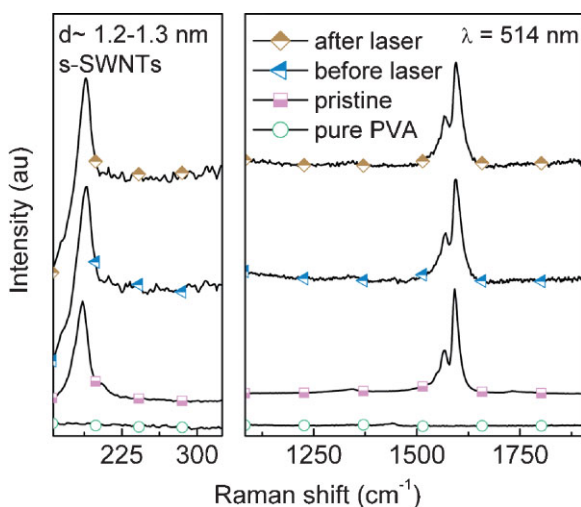


Figure 8. Raman spectra of SWNTs embedded in PVA before and after their operation in a laser cavity.

nanotubes–polymer composite prior and after usage as SA, for 12 h. We observe no change in $I(D)/I(G)$, implying that the nanotubes in the composite are not damaged due to laser irradiation.

6.3.4. PL Spectroscopy

PL can be observed from isolated SWNTs or small bundles,^[62,66,67] even when they are embedded in composites.^[201] However, for large bundles in dispersions or in composites, no PL is observed, as m-SWNTs provide nonradiative relaxation channels.^[62,302] SWNT-based SAs require the tubes in small sub-micrometer bundles. Therefore, PL spectroscopy could be used to confirm the presence of isolated SWNTs or small bundles.^[96]

6.3.5. Pump-Probe Spectroscopy

Pump-probe spectroscopy can be used to characterize SAs.^[32] By studying the transmission or reflection of the probe pulse, it is possible to obtain information on the excitation decay (recovery time of the SA) caused by the pump pulse. For SWNT-based SAs, generally, a biexponential response, composed of a fast and a slow decay, is observed.^[188,303] These are due to different time-scale relaxation processes (interband and intraband, respectively).^[304,305] As an example, we have recently studied commercially available SWNT (Carboxex Inc.) films with a maximum absorption centered at 1.9 μm using sub-100-fs two-color pump-probe spectroscopy.^[188] We found that these SWNTs, spray-coated on a quartz substrate, have a 370 fs relaxation time^[188]. This shows that they are ideal to passively mode-lock Tm and Ho lasers at ~ 2 μm .^[188,306]

6.3.6. Z-Scan and Power-Dependent Transmission

Z-scan experiments probe the optical nonlinearities associated with the change in refraction and absorption coefficient induced by intense laser power.^[84,185,307–310] The material is moved along the waist of a Gaussian beam, as shown in Figure 9a. This results in a variation of the laser-power density on the sample, which reaches its maximum at the focal point. An analysis of the transmitted beam through the sample as a function of the sample position, Z , is carried out either in the open or in the close-aperture scheme.^[307–309] Open-aperture Z-scan is used for the investigation of processes associated with nonlinear absorption, while close-aperture Z-scan is used to investigate nonlinear refraction.^[307]

A normalized Z-scan trace for a SWNT–polymer composite, taken in near resonant conditions, is plotted in Figure 9b. Here, SWNTs show strong saturable absorption with $\sim 30\%$ increase in transmission when the sample passes the focal point.

Although not as accurate as Z-scan, power-dependent transmission may also be used to study saturable absorption,^[98,125,185] as shown in Figure 10a. By means of a variable optical attenuator, the input power to the composite is varied. A reference signal is taken using a coupler to measure the incident power. In contrast to Z-scan, power-dependent measurements do not need a free-space setup. A small composite (typically ~ 2 mm^2) can be directly integrated between fiber connectors. Figure 10b shows normalized

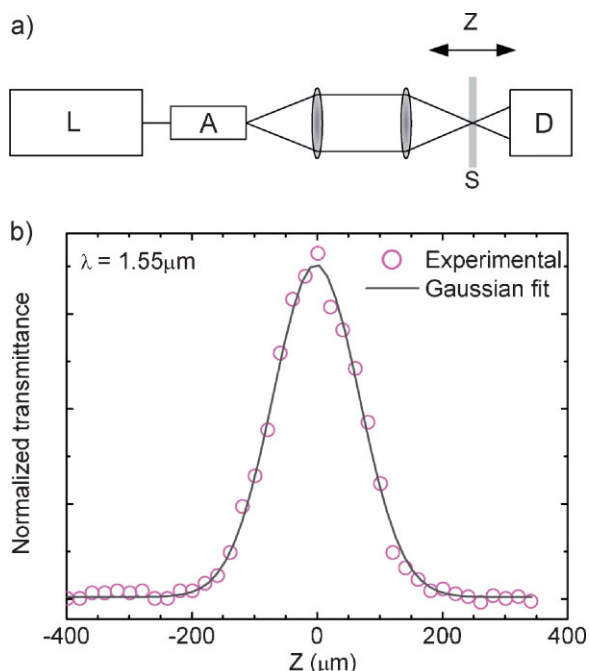


Figure 9. a) Z-scan setup. L: laser, A: attenuator, D: photodetector, S: sample. b) Z-scan measurement of a SWNT-polymer composite showing change in transmittance due to change in incident laser intensity.

power-dependent absorption measurements of a SWNT-polymer composite. The absorption decreases as the input intensity increases. The composite shows $\alpha_0 \approx 13\%$ and $\alpha_{ns} \approx 87\%$. Ideally, the absorption at low input intensity should be small with a large modulation depth, i.e., power-dependent change in transmission (ΔT).

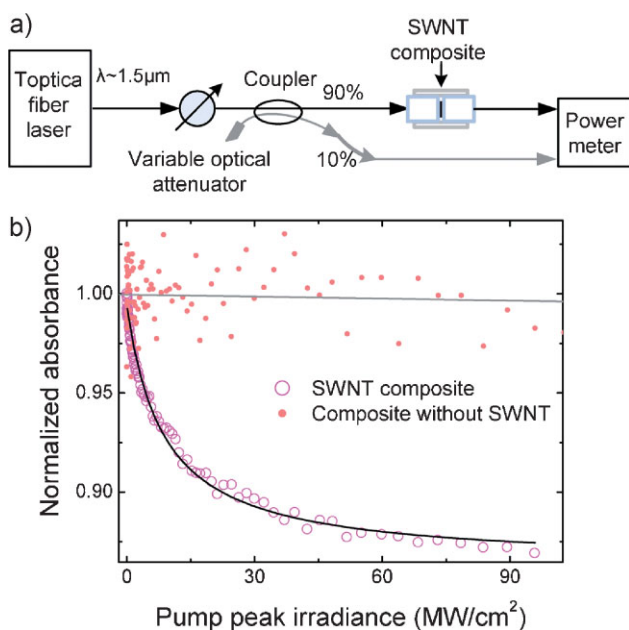


Figure 10. a) Experimental setup for power-dependent transmission measurements. b) Normalized absorption of a SWNT-polymer composite as a function of pump-pulse peak intensity at 1550 nm.

7. Nanotube Composites as Mode-Lockers for Ultrafast Lasers

Mode-locking is a very effective method to generate ultrafast laser pulses.^[30,32,174] In general, at any given time, the relative phases between oscillating laser modes randomly fluctuate.^[30,32,174] If no fixed-phase relationship exists, the laser output varies in time, although the average power remains relatively constant.^[32] Locking modes in phase, i.e., mode-locking, can result in a train of short pulses, temporally spaced by well-defined periods.^[32] Mode-locking techniques can be classified either as active or passive.^[30,32,174]

Active implies external modulation of amplitude or phase of the oscillating light, with a repetition rate matched to the cavity round trip time.^[30,32,174] This may be achieved by inserting an acousto-optical or electro-optical modulator inside the cavity.^[30,174]

Passive mode-locking involves self-amplitude modulation, provided by an intracavity passive nonlinear device having high loss at low intensity and low loss at high intensity, i.e., a SA material.^[30,32,174] Therefore, the loss modulation is provided by the intracavity intensity itself, rather than being externally controlled. This can generate shorter pulses, as self-modulation can provide much stronger pulse-shaping than any active electronic modulator.^[30,32,174] More specifically, a SA works in the cavity as an optical discriminator, transmitting optical pulses with intensity higher than a certain threshold and suppressing those below.^[30,32,174] When the absorber is saturated, the overall cavity gain exceeds the loss, enabling transmission of short pulses. Then the recovery of the SA restores the intracavity loss to a level higher than the gain, preventing lasing during the rest of the round-trip time.

To date, SWNT-based SAs have been successfully used as mode-lockers in fiber lasers,^[94,96–98,145–148,153,156,186,191] waveguide lasers,^[95] solid-state lasers,^[149,150,189,311,312] and semiconductor lasers^[155] at 1, 1.3, 1.55, 1.6,^[97] and 1.9 μm .^[152,207,313] A list of SWNT-based mode-lockers, their performance ranges, and specifications is presented in Table 1. The mode-lockers are broadly classified according to the means of device integration. In 2003, the authors of Ref. [182] first introduced spray-coated SWNT devices for mode-locking. Later, SWNT solutions^[314–316] and direct growth/transfer of SWNTs on substrates^[184,207,323–325] were also used. However, the abovementioned methods have a number of disadvantages. For example, the spray-coated or as-grown/transferred SWNTs on various substrates utilize exposed SWNTs. In addition to being highly moisture-absorptive, these devices can also be physically unstable.^[328] They also contain aggregates with dimensions compared to the device-operation wavelength. These cause unwanted scattering losses. The solutions are inherently unstable, and introduce additional scattering losses from aggregates and bubbles. SWNTs embedded in polymer matrices were first employed as SAs.^[83] This approach avoids the disadvantages of other methods. For example, SWNTs can be embedded homogeneously in sub-micrometer bundles, avoiding unwanted scattering losses. Also, wet-chemistry-based processing allows easy and economic integration into various photonic systems. Different polymer matrices have been introduced to address various issues, in particular, transparency at device-operation wavelength and

Table 1. Lasers mode-locked by carbon nanotubes.

Type of mode-locker		Type of SWNTs	Laser type	Operation wavelength, nm	Typical Laser specifications		
					Pulse width	Repetition	Average power
SWNT solution	Solution in D ₂ O	HiPco ^[314,315]	F ₂ :LiF ^[315] , Er:glass ^[314]	1540 ^[314] , 1150 ^[315]	< 1 ns ^[314]	//	//
	SWNT-filled microchannel	HiPco ^[316]	EDF ^[316]	1566 ^[316]	2.3 ps ^[316]	2.56 MHz ^[316]	22.4 mW ^[316]
Grown/ deposited/ transferred SWNTs	Optically driven deposition	HiPco ^[317,318]	Er ^[317,318,320]	1070 ^[317] , 1560 ^[317,318] , 1563 ^[320]	137 fs ^[317]	20.1 MHz ^[317]	0.1 mW ^[317]
		CoMoCAT ^[317]	Yb ^[317] -doped fiber		1.06 ps ^[318]	81.7 MHz ^[317]	1.5 W ^[318]
	on fiber end Spray coated	HiPco ^[154,321] , CVD ^[149,151,155,322,319]	Pr ^[321] , Tm ^[151]	1294 ^[321] , 1506 ^[151] , 1550–1571 ^[145,149,151]	261 fs ^[149] , 14 ps ^[155]	3.18 MHz ^[321] , 17.2 GHz ^[155]	16 μW ^[155] , 63 mW ^[149]
		Laser ablation ^[145]	Er:Yb ^[319] -doped fiber, Solid-state Er:Yb: glass ^[149] , Semiconductor laser ^[155]	1605 ^[151]			
Grown/ transferred	Alcohol catalytic CVD ^[184,323–325] , Catalytic CO disproportionation reaction ^[207]	Yb ^[207] , Er ^[184,207,323–325] , Tm ^[207]	1050 ^[207] , 1560–1565 ^[184,207] , 1990 ^[207]	440 fs ^[207] , 1.14 ps ^[325]	6.62 MHz ^[325] , 50.4 MHz ^[184]	22 μW ^[325] , 250 mW ^[324]	
		-doped fiber					
SWNT-polymer Composite	NaCMC composite	CoMoCAT ^[150] , HiPco ^[189]	Nd:glass ^[150] , Nd:GdVO ₄ ^[189]	1000 ^[150] , 1340 ^[189] , 1555 ^[153] , 1930 ^[152]	177 fs ^[153] , 30 ps ^[189]	37 MHz ^[152] , 50 MHz ^[153]	3.4 mW ^[152] , 7 mW ^[153]
		Arc discharge ^[152,153]	and Nd:Y _{0.9} Gd _{0.1} VO ₄ solid state glass ^[189] , Er ^[153] , Tm ^[152] -doped fiber				
	Polyimide composite	Laser ablation ^[124,150]	Er:glass solid state ^[150] , Er ^[124] -doped fiber laser	1565 ^[124] , 1570 ^[150]	68 fs ^[150] , 165 fs ^[124]	23.2 MHz ^[124] , 85 MHz ^[150]	1.2 mW ^[124] , 80 mW ^[150]
			HiPco ^[146,326]	Yb ^[191] , Er ^[146,326,327] -doped, Tm-Ho ^[313] co-doped fiber laser	1035 ^[146,191,327] , 1885 ^[313]	235 fs ^[191] , 1.5 ps ^[191]	13.3 MHz ^[146] , 50 MHz ^[191]
	PMMA composite	HiPco ^[99,102,311] , Arc discharge ^[312]	Yb:KLuW ^[312] , Cr:forsterite solid state ^[311] , Er ^[99,102] -doped fiber	1048 ^[312] , 1250 ^[311] , 1560 ^[102] , 1562 ^[99]	115 fs ^[312] , 1.9 ps ^[99]	5.3 MHz ^[99] , 89 MHz ^[312]	50 μW ^[102] , 202 mW ^[311]
			Er-doped fiber ^[101]	1560 ^[101]	147 fs ^[101]	51 MHz ^[101]	4.1 mW ^[101]
	PC composite	HiPco ^[100] , Laser ablation ^[96,98]	Er-doped fiber ^[96,98,100]	1518–1558 tunable ^[98] , 1560 ^[96,100]	115 fs ^[100] , 2.4 ps ^[98]	15 MHz ^[98] , 39 MHz ^[100]	0.36 mW ^[98] , 3.4 mW ^[100]
			CoMoCAT ^[157] , Laser ablation ^[94,95,97]	Yb ^[157] , Er ^[94,97,125,147,148,156,158] -doped fiber, waveguide ^[95]	1060 ^[157] , 1532–1563 ^[94,95,125] , 147, 148, 156, 158, 159, 186 ^[95] , 1601 ^[97]	123 fs ^[159] , 20 ps–2 ns, selective ^[157]	177 kHz–21 MHz, selective ^[157] , 26.7 MHz ^[97]
	P3HT composite	HiPco ^[101]	Er-doped fiber ^[101]	1560 ^[101]	147 fs ^[101]	51 MHz ^[101]	4.1 mW ^[101]
	PVA composite	HiPco ^[100] , Laser ablation ^[96,98]	Er-doped fiber ^[96,98,100]	1518–1558 tunable ^[98] , 1560 ^[96,100]	115 fs ^[100] , 2.4 ps ^[98]	15 MHz ^[98] , 39 MHz ^[100]	0.36 mW ^[98] , 3.4 mW ^[100]

thermal, chemical, and environmental stability. Due to the ease of integration of SWNT–polymer SAs into photonic systems, the study of different device structures, for example using evanescent interactions^[146,191,313,327] or waveguide structures,^[95,124] has been pursued.

Performance-wise, the shortest pulse duration thus far achieved is 68 fs by a mode-locked Er/Yb:glass laser.^[150] The authors of Ref. [150] implemented a SWNT–polyimide composite

as SA with maximum absorption centered at around 1500 nm in a Er/Yb:glass solid-state laser.^[150] A repetition rate of 17.2 GHz was demonstrated in Ref. [155]. The maximum output power reported to date is 1.6 W.^[158] To realize various functions, different configurations of SWNT-based SAs have been proposed, such as evanescent-field interaction in a tapered fiber,^[146,154,191,313,327] in a D-shaped optical fiber,^[322] and with vertically aligned SWNTs.^[323] Nevertheless, as seen from Table 1, compared to

solution or growth/transfer/deposition, the vast majority of published literature focuses on SWNT–polymer SAs, due to the inherent flexibility in the SWNT–polymer device fabrication and ease of integration into the laser cavity. In the following, we mainly review the advances of nanotube–polymer composites for ultrafast pulse generation.

7.1. SWNT–Polymer Mode-Locked Solid-State Lasers

The term “bulk solid-state laser” refers to a laser with a bulk piece of doped crystal or glass as the gain medium, and discrete laser mirrors placed around the crystal (or glass).^[30] The beam propagates in free-space between the gain medium and mirrors. For mode-locking using SWNT-based SAs, various gain media have been utilized at different wavelengths.^[149,150,311,312,314,315] SAs are usually deposited onto an optical component.^[99] This can be achieved by spin coating, and allows mode-locking of monolithic cavities, for example microchip lasers or nonplanar ring oscillators when the SA is directly applied on the laser crystal.^[150] After spin coating, post-processing, such as application of antireflection, partial-reflection, or high-reflection coatings is possible.^[150] The SAs are then inserted into the air space with reflective- or transmission-type structures, see Figure 11a^[150] and b.^[312] As solid-state lasers allow much lower single-pass gain (<10),^[30] low insertion loss is critical for the SA design. This can be controlled by the film thickness or SWNT concentration.^[312,329]

SWNT–polymer composites were used as reflective SAs in Ref. [150], where a thin SWNT–polymer composite was placed onto a fused-silica dielectric mirror. This was coated with a TiO₂/SiO₂ dielectric film, providing broad reflectivity bandwidth. Using such mirrors, stable self-starting mode-locking (starting from noise after turn-on of pump power) with pulse durations in the femto- and picosecond regimes, was achieved.^[150] The gain media were Nd:glass and Er/Yb:glass, with output wavelengths at 1 and 1.5 μm, respectively. The authors of Ref. [149] also demonstrated spray-coating of SWNT onto 30 pairs of anti-resonant AlAs/GaAs-distributed Bragg reflector mirrors. This quasi-antiresonant design was used to enhance the interaction between the SWNTs and pump light.^[149] SWNT–polymer composites have also been deposited directly onto a quartz substrate to form a transmission-type SA structure.^[311,312] Using this, mode-locked Yb:KLuW and Cr:forsterite lasers were demonstrated with nearly transform-limited pulses as short as 115 fs (at 1 μm) and 120 fs (at 1.25 μm), respectively.^[311,312]

7.2. SWNT–Polymer Mode-Locked Fiber Lasers

The development of compact, diode-pumped, ultrafast fiber lasers as alternative to bulk solid-state lasers is fast progressing because of their simplicity, compactness, efficient heat dissipation, and alignment-free waveguide format.^[21,45,330–333] Thus far, fiber lasers are the most commonly mode-locked with SWNTs,^[94,96–98,145–150,153,155–159,186,189,191] due to the ease of coupling SWNT–composites into a fiber laser. In addition, they normally require large modulation depths in order to stabilize the

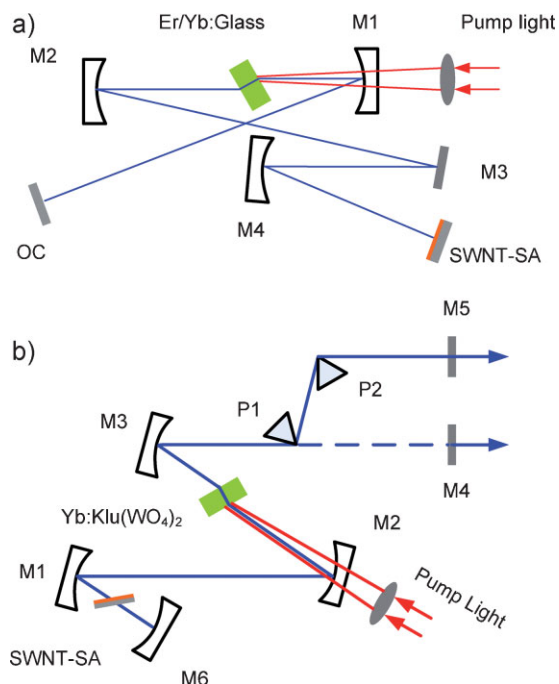


Figure 11. Schematics for a) SWNT-SA mode-locked bulk solid-state laser with reflective type structure; b) SWNT-SA mode-locked bulk solid-state laser with transmission type structure. Er/Yb:Glass, gain medium; M1, M2, M3, and M4, optical mirrors; OC, Output coupler; P1, P2, prisms. Adapted from [150,312].

intracavity pulses,^[45] which can be provided by the relatively large nonlinearity of the SWNT mode-locks. It should also be noted that for fiber lasers, the single-pass gain is appreciably larger (several tens of dB) than solid-state gain media. Therefore, nonsaturable losses are not a major issue.^[98,149]

A range of polymer matrices have been used as the host for SWNTs.^[96,97,100–102,152,153] The performance of fiber lasers mode-locked by SWNT composites is quickly approaching that achieved with conventional techniques using SESAMs. The spectral coverage of SWNT-enabled fiber lasers is superior to that of conventional SESAMs, especially for the ≥ 1.3 μm spectral range. The SWNT SAs operating band can be selected by varying the mean tube diameter.^[152,207,313,317,321] So far, SWNT-based SAs have successfully mode-locked Yb-doped (~1 μm),^[207,317] Pr-doped (~1.3 μm),^[321] Er-doped (~1.5 and 1.6 μm),^[96,97,125,147,156,207] and Tm-doped (~2 μm)^[152,207,313] fiber lasers.

7.2.1. SWNT Mode-Locked Soliton Fiber Lasers

To date, most passively mode-locked fiber lasers have employed the soliton effect^[21,332–335] for short pulse generation. However, a detailed study of the mode-locking dynamics is still missing.

In this regime, near-transform-limited pulses preserving temporal and spectral shape (i.e., behaving like solitons^[21]) circulate in a cavity with anomalous group-velocity dispersion (GVD).^[21] Anomalous GVD facilitates soliton-pulse shaping, through the interplay of GVD and self-phase modulation (SPM), i.e., the phase modulation caused by the pulse’s own

intensity.^[21,32] This type of laser is called a soliton fiber laser.^[336] The soliton period Z_0 is defined as:^[21]

$$Z_0 = \frac{\pi}{2} L_D = \frac{\pi}{2} \frac{T_0^2}{|\beta_2|} \approx \frac{T_{FWHM}^2}{2|\beta_2|} \quad (4)$$

where T_0 is the pulse's half-width at $1/e$ -intensity, β_2 is the second-order dispersion coefficient, and L_D is the dispersion length defined by:

$$L_D = \frac{T_0^2}{|\beta_2|} \quad (5)$$

For soliton fiber lasers, the nonlinear phase shift in one round-trip is determined by the pulse energy and width.^[21] This limits the energy achievable with a soliton of given width, since overdriven nonlinear phase shifts tend to cause instability.^[337–339]

Another mechanism that may adversely affect mode-locking is side-band generation, where the energy of the soliton pulses is resonantly coupled into the accompanying dispersive waves.^[21,340] These give discrete and well-defined peaks in the optical spectrum of the soliton pulses.^[340] When the power of these dispersive waves reaches the lasing threshold, they tend to deplete the gain of the laser, and subsequently destabilize mode-locking.^[341,342]

To clarify the applicability of SWNT–polymer composite SAs in mode-locked ultrafast fiber lasers and to provide insights on the design guidelines for such devices, we assembled a fiber ring cavity comprising a 9.7 m fiber with mean cavity dispersion $\beta_{2,ave} = -27.5 \text{ ps}^2 \text{ km}^{-1}$.^[156] In addition, to get the shortest pulse, we also measured the mode-locking dynamics while increasing the pump power.^[156] The mode-locker used in the cavity was a $\sim 50 \text{ }\mu\text{m}$ SWNT–PVA composite with modulation depth, I_{sat} , and α_{ns} of 16.9%, 18.9 MW cm^{-2} , and 82.5%, respectively. Self-starting mode-locking was observed at a pump power of 40 mW. Figure 12a and b show the dynamic change of the optical spectra and output autocorrelation traces when the pump power is increased. At 58.2 mW, we achieved a pulse duration of ~ 640 fs. When pumping was further increased, the output became unstable and the pulse broke into multiple uncontrolled pulses. Both temporal and spectral trends shown in Figure 12a and b confirm soliton operation.^[156] The threshold pump power (~ 60 mW) for single-pulse per round-trip mode-locking coincides with observation of spectral instability (i.e., the generation of sub-sidebands). This strongly indicates that the growing strength of the dispersive wave may be the mode-locking destabilizing factor.^[343] Generally, soliton sideband generation arising from periodic cavity perturbations plays a major role in limiting the stability of fiber ring lasers when $L = 1Z_0$ or $2Z_0$ (where L and Z_0 are the cavity length and soliton period, respectively)^[334,336] or the nonlinear phase shift per cavity round-trip approaches $3\pi/2$.^[337] Assuming a 600 fs average pulse duration inside the cavity, the soliton period, as defined by Equation 4, is $Z_0 = 6.55$ m. This gives $L = 1.48 Z_0$. The nonlinear phase shift is more difficult to estimate, since the pulses experience discrete loss and gain within the cavity. The soliton power before and after the output coupler is used to estimate the upper and lower limits of the average soliton peak power. This gives a nonlinear phase shift of 1.1π – 2.3π per

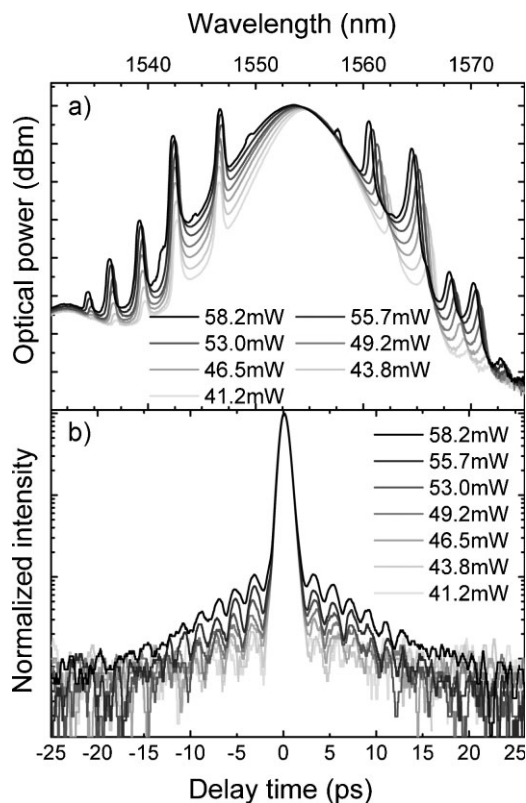


Figure 12. a) Output spectra. b) Output autocorrelation traces at seven different pump levels (41.2, 43.8, 46.5, 49.2, 53.0, 55.7, and 58.2 mW).

round trip, and confirms that sideband generation and overdriven nonlinearities, rather than the SWNT mode-locker, are the limiting factors for this laser.

7.2.2. SWNT–Polymer Mode-Locked Stretched-Pulse Fiber Lasers

Pulse durations of 115 fs at 1550 nm^[100] and 137 fs at $1 \mu\text{m}$ ^[317] were reported for soliton-like operation, with the majority of mode-locked soliton fiber lasers giving pulses between 200 fs and 1 ps.^[94,96–98,145–148,153,156,186,191] Enhanced nonlinearity due to strong confinement of the propagating mode and long interaction distance in the fiber cavity are believed to prevent the generation of sub-200 fs pulses.^[337–339] To overcome this restriction, a dispersion managed cavity, known as stretched-pulse, based on fibers with alternating dispersion, may be used.^[336]

As shown in Figure 13, a stretched-pulse fiber laser uses segments of fiber with large positive (group velocity increasing with decreasing frequency) and negative (group velocity increasing with increasing frequency) dispersion, whereby a small positive overall GVD is achieved.^[336–339,344] The pulse maintains minimum duration only over portions of fiber, and accumulates less nonlinear phase shift. This reduces the nonlinear phase shift, creating pulses with larger energies than those in the soliton regime.^[336]

We designed a stretched-pulse fiber ring cavity using fibers of alternating dispersion.^[187] A Er^{3+} fiber with an estimated dispersion of $\beta_2 = +36 \text{ ps}^2 \text{ km}^{-1}$ was the gain medium. The rest of the laser was constructed from Flexcor 1060

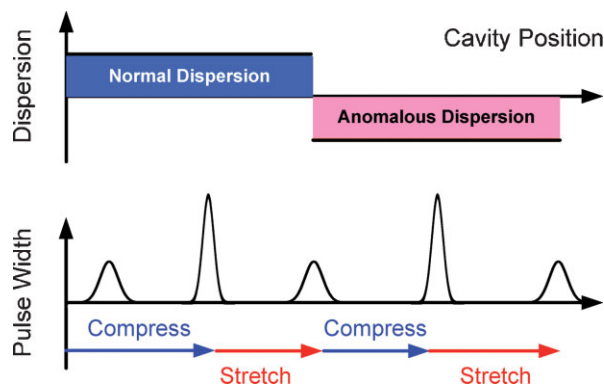


Figure 13. Simplified schematic of stretched-pulse fiber laser with the intracavity dispersion map (above) and pulse-width distribution (below). Normal (positive) and anomalous (negative) dispersion are marked with different colors [159].

($\beta_2 = -7 \text{ ps}^2 \text{ km}^{-1}$) and Corning SMF28 ($\beta_2 = -22 \text{ ps}^2 \text{ km}^{-1}$) fibers with negative dispersion. Their length was adjusted so that the total intracavity GVD was $\sim(-0.008 \pm 0.005) \text{ ps}^2$. Self-starting mode-locking was observed at a pump power of $\sim 12.8 \text{ mW}$.^[187] Figure 14a shows an output spectrum with a central wavelength of $\sim 1560 \text{ nm}$. Unlike soliton fiber lasers, no sidebands are observed. Figure 14b plots the autocorrelation traces of the output pulses after passing through different lengths of external GVD patchcords. Assuming a Gaussian temporal profile, typical of stretched-pulse lasers,^[336,338,339] the data deconvolution gives a $\sim 123 \text{ fs}$ pulse after 0.003 ps^2 fiber patchcord, and a $\sim 961 \text{ fs}$ pulse after -0.03 ps^2 . This indicates that the output pulse stretches approximately eight times after the $\sim 0.033 \text{ ps}^2$ fiber. Considering the pulse evolution and the -0.096 ps^2 intracavity fiber between the coupler and the EDF, the stretched-pulse design is confirmed. It should be noted that the wider and cleaner spectrum (full-width at half-maximum, FWHM, $\sim 32 \text{ nm}$) from our laser implies the possibility to get sub-100 fs pulses. The pulse duration is likely limited by the uncompensated third-order dispersion (TOD) of the cavity.^[21,345] Since the TOD is typically proportional to the fiber length, by reducing it, shorter pulses may be obtained.

7.2.3. SWNT Mode-Locked Tunable Fiber Lasers

Ultrashort-pulse lasers with spectral-tuning capability have widespread applications in spectroscopy, biomedical research, and telecommunications.^[335] The inclusion of a broadband SA can offer tunability over a range of wavelengths, unlike SESAMs.

Compared to SESAMs, SWNT-based SAs possess a much wider operating range^[97,98,207,313] due to the inherent inhomogeneity of diameter (band gap) in as-prepared SWNT samples. To realize tunable fiber lasers using SWNT-polymer SAs, we fabricated a $\sim 40 \mu\text{m}$ thick SWNT-PC composite with a broad absorption band ($\sim 300 \text{ nm}$) centered at $1.55 \mu\text{m}$ ^[98] using SWNTs of 1–1.3 nm diameter, covering the S, C, L, and U bands, as shown in Figure 15.^[346] Figure 16 plots the power-dependent transmission of the composite. The modulation depth and saturation intensity are 12% and 5.8 MW cm^{-2} , respectively.^[98] The very slight change of modulation depth implies an operating range much larger than 30 nm.

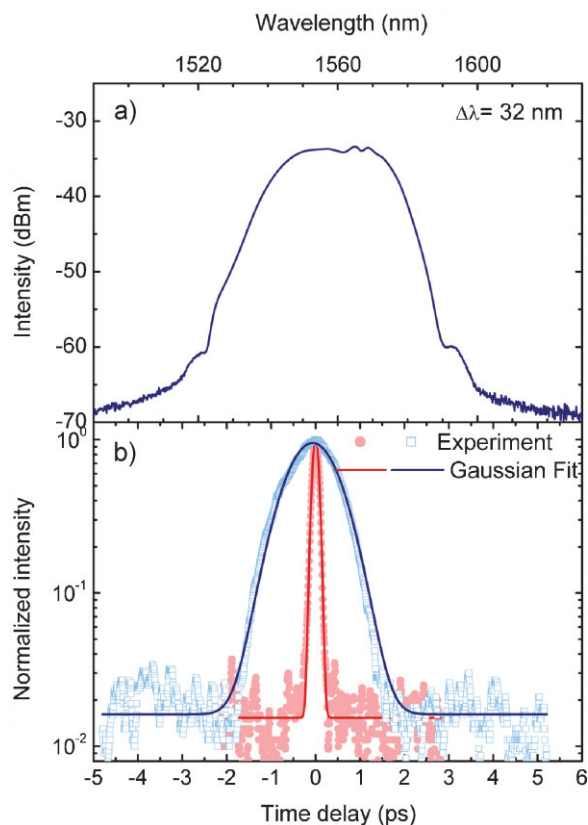


Figure 14. a) Typical output spectrum of a stretched-pulse laser cavity. Center wavelength $\sim 1.56 \mu\text{m}$ and FWHM $\sim 32 \text{ nm}$. b) Autocorrelation traces of output pulses after $\sim 0.003 \text{ ps}^2$ (solid circles) and $\sim (-0.03) \text{ ps}^2$ (open squares) fiber patchcords.

The schematic of the tunable fiber ring cavity is shown in Figure 17. We achieved the best tuning results when the SWNT-PC mode-locker was placed at the input of the gain fiber. When the SWNT mode-locker is not present, CW lasing could be extended from 1518 to 1565 nm by feeding more pump power to the Er^{3+} fiber. A tuning range of 40 nm (1518–1558 nm) is possible in this setup.^[98] Figure 18a illustrates the output autocorrelation traces and spectra at several wavelengths. The pulses are expected to have a sech^2 shape.^[21] This gives an average pulse duration of $\sim 2.39 \text{ ps}$ over the tuning range. By employing a tunable filter with larger pass-band, shorter pulses may be obtained.^[344] Figure 18b shows the spectra at different center wavelengths. They stay fairly flat over the 40 nm tuning range. The soliton sidebands are suppressed as a result of the spectral filtering effect of the intracavity filter.^[344] For comparison, the laser output when no filter is present is shown in Figure 18b. The output pulse is now 706 fs, and soliton sidebands appear because of periodic cavity perturbations.

Note that the operating bandwidth of SWNTs is not the limiting factor for tunability. In principle, this setup could enable tuning for other bands, such as S (1460–1530 nm) and L (1565–1624 nm), if gain fibers and tunable filters at these wavelength ranges were available. Recently, a single SWNT SA device was used to demonstrate mode-locking of three lasers at discrete wavelengths spanning $1 \mu\text{m}$ (from $\sim 1 \mu\text{m}$ to $\sim 2 \mu\text{m}$).

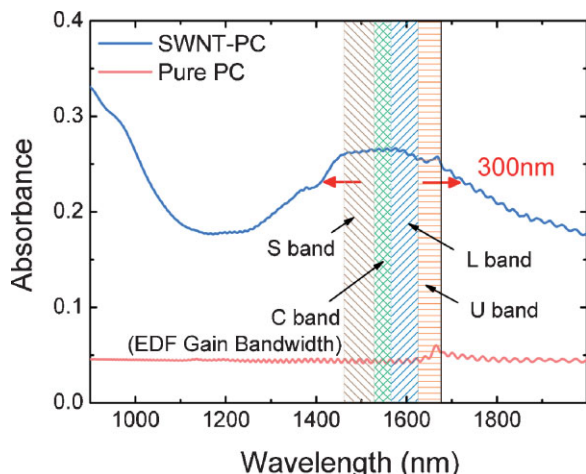


Figure 15. Absorption spectra of a SWNT-PC composite and pure PC. The stripes show the telecommunication windows that can be potentially covered by this composite. S band: 1460–1530 nm, C band: 1530–1565 nm, L band: 1565–1625 nm and U band: 1625–1675 nm. Adapted from [98].

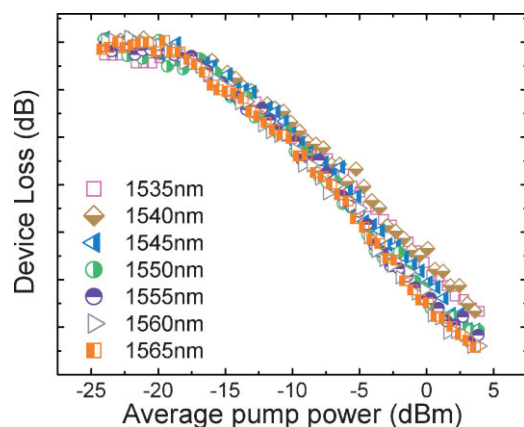


Figure 16. Power dependent absorption measurement of a SWNT SA composite at seven different wavelengths. The pump power ranges from $\sim 3 \mu\text{W}$ to $\sim 3 \text{ mW}$.

This again confirms the ultrawide operating bandwidth of SWNT SAs.^[207]

7.2.4. Power Scaling in SWNT-Polymer Mode-Locked Fiber Lasers

The scaling of output power is key to developing fiber-laser systems for micromachining, surgery, and other applications.^[24,31,32,45,335] High output power can be achieved with solid-state lasers.^[149,150] By using a SWNT-polyimide SA mirror, an average output power of up to 80 mW was reported for an Er/Yb:glass solid-state laser.^[150] Higher powers for SWNT mode-locked fiber lasers were achieved using non-transmissive SAs.^[146,154,191,322–324] Unlike conventional transmissive type devices, these employ evanescent-field interaction with SWNTs.^[324] By using a tapered fiber embedded in a SWNT-polydimethylsiloxane composite, 594 fs pulses with an average power of 23 mW (1.7 nJ pulse energy) were demonstrated in

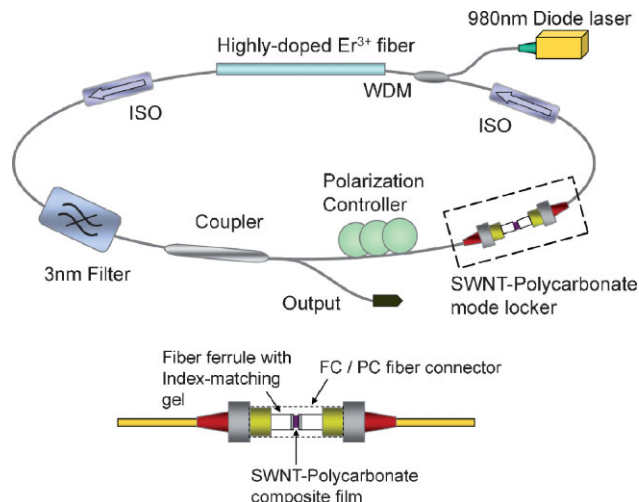


Figure 17. Laser setup and mode-locker assembly. This schematic shows the standard fiber-optic components, such as an optical isolator (ISO), a wavelength division multiplexer (WDM), a coupler, and a polarization controller. The total length of the cavity is $\sim 13.3 \text{ m}$. Adapted from [98].

Ref. [146]. The use of vertically aligned SWNTs grown on a D-shaped fiber allowed an output power of 250 mW (6.5 nJ pulse energy) for $\sim 1 \text{ ps}$ pulses.^[324] An all-fiber version of normal-dispersion laser was reported, generating 1.5 ps, 3 nJ pulses that could be compressed to 250 fs duration outside the cavity by dispersion compensation.^[191]

Alternatively, the power can be boosted by adding an amplifier, such that it becomes a master oscillator power amplifier (MOPA) system.^[30,318] We believe this to be the best solution to overcome the limitations set by the overdriven nonlinearity caused by increased power within the laser cavity. Using a MOPA mode-locked by SWNT-based SAs, we achieved 1.6 W average output power at 1550 nm, corresponding to energy per pulse of 65 nJ.^[158]

Recently, we also demonstrated selectable pulses with durations ranging from 20 ps to 2 ns at repetition rates between 21 MHz and 177 KHz in a passively mode-locked Yb fiber laser with a SWNT-based SA.^[157] The output pulses are over 600 times their transform-limited duration, which could be used for a simplified chirped-pulse amplification system capable of producing an output of 10 W or even higher.^[158] This is very promising for commercial and industrial applications, as it can provide a cheap, compact, and stable system.^[23,157,158,335]

7.3. SWNT-Polymer Mode-Locked Waveguide Lasers

Passive mode-locking of waveguide lasers is interesting due to their inherent simplicity and compactness.^[95] For example, Er/Yb-doped-glass waveguides can produce large gains over very short lengths, allowing compact cavities and high repetition rates.^[95,335] Such lasers could generate low-noise and inexpensive light sources for applications in optical communications, optically sampled analog-to-digital converters, etc.

We demonstrated mode-locking in an active waveguide laser manufactured by femtosecond laser writing.^[95] This is a simple and inexpensive technique that avoids any photolithographic process and allows three-dimensional fabrication. After laser

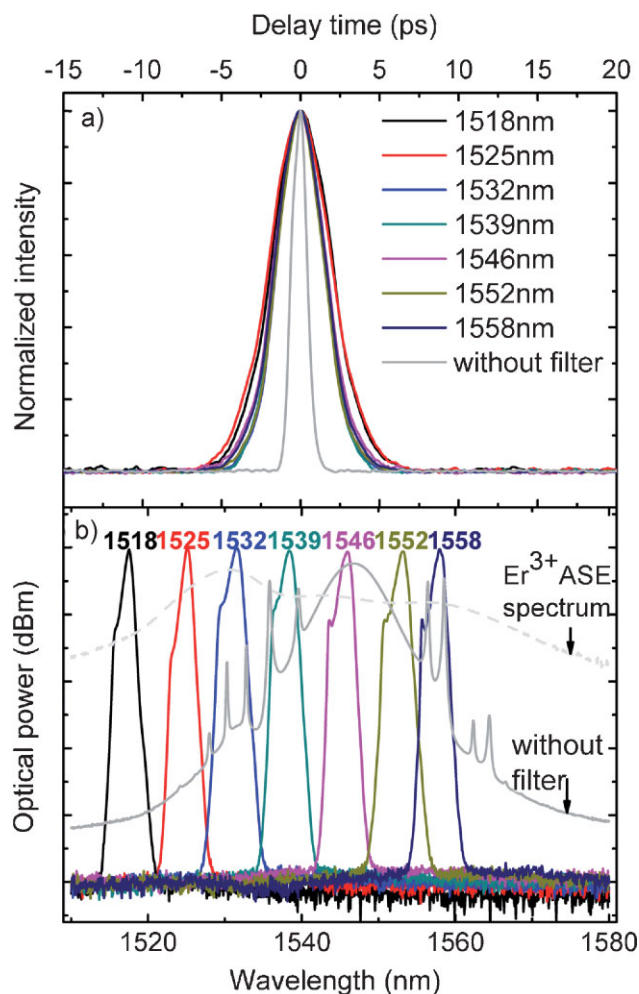


Figure 18. a) Autocorrelation traces of laser output at different central wavelengths (dashed line, laser output without bandpass filter). All traces do not show pedestals (low-intensity backgrounds), indicative of single-pulse operation and reflection-free design. b) Output spectra at seven different wavelengths.

inscription, both end-facets of the waveguides were polished. A 36-mm-long waveguide with insertion losses of 1.9 dB ($\sim 65.5\%$) was used.^[95] Broad net gain over the whole C band was observed, with 7.3 dB peak gain at 1535 nm for an incident pump power of 460 mW. A schematic is shown in Figure 19. The SWNT polymer composite was packaged by sandwiching the film in the fiber pigtailed FC/PC connector with index-matching gel at both fiber ends. The autocorrelation trace had an FWHM of 2.72 ps, corresponding to a pulse duration of 1.76 ps, indicating transform-limited output pulses. The carrier-to-noise ratio of 65 dB ($10^{6.5}$ contrast) showed low timing jitter (deviation of the temporal pulse positions from those in a perfectly periodic pulse train) from the radio-frequency spectrum.^[347]

An upgraded version of this technology, using the same waveguide gain section with SWNTs incorporated into a monolithic laser structure, could provide very compact sources with high repetition rates of up to 3 GHz. An even higher

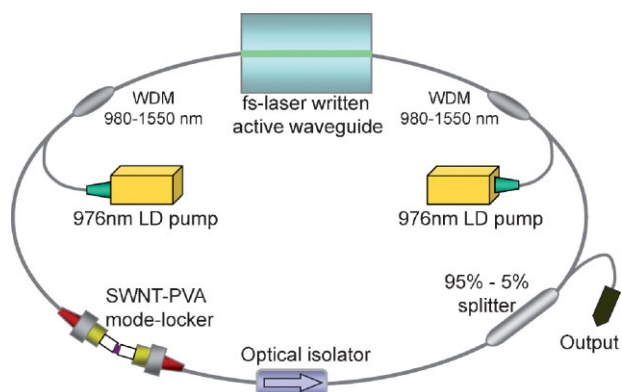


Figure 19. Schematic setup of a waveguide laser cavity configuration. Adapted from [95].

repetition rate could be achieved by decreasing the length of the waveguide gain section.^[95,348]

8. Graphene–Polymer Composites as Mode-Lockers for Ultrafast Lasers

Graphene is the latest carbon allotrope discovered, and it is now at the center of a significant research effort.^[349–355] Near-ballistic transport at room temperature and high mobility^[354–359] render it a potential material for nanoelectronics,^[360–363] especially for high-frequency applications.^[364] Furthermore, its transparency and mechanical properties are ideal for micro- and nanomechanical systems, thin-film transistors, and transparent and conductive composites and electrodes.^[365–368]

A single graphene layer absorbs $\sim 2.3\%$ per layer in the visible–IR excitation range, and this scales linearly with the number of layers until ~ 6 – 10 layers.^[369–371] It is thus immediate to consider if this could be a viable material for mode-locking. The ultrafast carrier dynamics of one and few-layer graphene was recently studied,^[372–374] yielding relaxation time constants comparable to those observed in nanotubes.^[82–86,373–376] Unlike SWNTs, the optical absorption spectra of chemically unmodified graphene is featureless from visible to near-IR.^[377] It is possible to reach saturable absorption for high-enough power, due to Pauli blocking.^[378] This, combined with the ultrafast carrier dynamics and large absorption of incident light per layer,^[369–371] makes one and few-layer graphene fast saturable absorbers from the visible to IR light range.

Following a solution-processing strategy similar to that for SWNTs,^[367] we have recently produced a polymer composite homogeneously embedding sub-micrometer flakes of single and few-layer graphene.^[378] We observed saturable absorption over at least a 20 nm range. Further characterization of wavelength tunability was only limited by our setup. We then tested mode-locking at 1550 nm using a fiber laser setup similar to the one shown in Figure 17, but without the tunable filter. Typical laser outputs are shown in Figure 20. The center wavelength is 1557 nm, with a 3.2 nm bandwidth, and pulse duration ~ 800 fs.^[378] The time–bandwidth product is 0.317, close to the theoretical value of 0.314 for Fourier-transform-limited sech^2

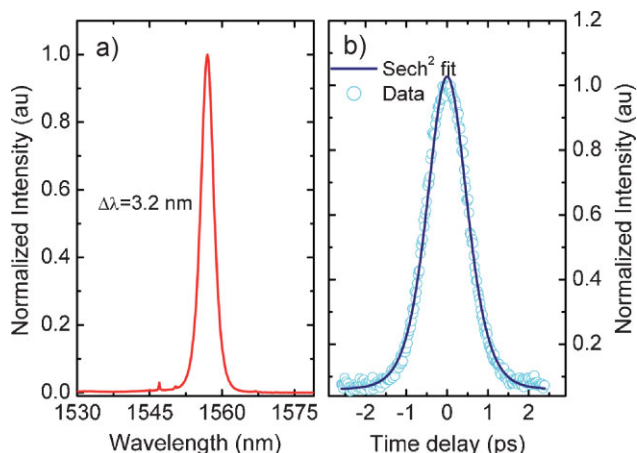


Figure 20. Graphene mode-locked laser performance: a) output spectrum, peaked at 1557 nm, b) output autocorrelation trace. The pulse duration is 800 fs. Adapted from [378].

pulses, indicating that the pulse is as short as allowed by the spectral bandwidth.^[21] Further cavity optimization, such as intracavity group dispersion management, could be used to achieve even shorter pulses. This composite is expected to mode-lock from visible to IR, due to the broad absorption range of graphene. For specific wavelength applications, however, the SWNT-based SAs, when optimized for diameter, are expected to have better performance.

9. Conclusions and Prospective

We reviewed the recent progress in the use of SWNT–polymer and graphene–polymer composites as saturable absorbers for generation of ultrashort laser pulses through passive mode-locking.

To date, planar, two-dimensional nanotube–polymer composites have mostly been used due to their ease of preparation. From materials to processing, SWNT–polymer composites hold great promise due to their inherent advantages in fabrication and device integration, and the prospective of easy integration in polymer-based photonics.

Graphene also shows saturable absorption due to Pauli blocking^[378] and can be deployed in mode-locked lasers, using a similar wet-chemistry strategy to SWNTs. Compared to SWNTs, graphene could have an ever broader operation and tunability range.

Thus far, only as-produced, heterogeneous nanotube samples randomly embedded in optical polymers have been used. The performance of these materials and the resulting devices is limited by the redundant, off-resonance tubes (whose band gaps are different from the device-operating wavelengths), as well as host polymers. Sorting/enrichment^[196,251,379–381] of SWNTs according to their diameter/band gap and electronic type opens the opportunity to further optimize device performance. For example, enriching a sample with (10,9),(12,7),(16,2),(17,0) tubes would be highly desirable for telecommunication applications specifically targeted at 1550 nm, since their eh_{11} absorption ranges from 1545 to 1561 nm.

The relaxation of excited states in s-SWNTs plays an important role in defining the pulse width. Since this is expected to decrease in the presence of m-SWNTs, tailored bundles of m-SWNTs and s-SWNTs could be created to optimize the devices.

Alignment of SWNTs is another potentially important strategy for better device performance, due to the high anisotropic interaction of SWNTs with light.^[382] In aligned SWNTs, absorption is maximum when polarization is parallel to the alignment direction.^[194,382] Alignment can be achieved by stretching the composite,^[194,201,280,383] or fabricating composites using the Langmuir–Blodgett technique.^[384–386] This can increase saturable absorption without increasing non-saturable losses.

Long-term stability and unwanted optical absorption/scattering from the host polymer are two other issues where significant improvement can be achieved. In this regard, silicone and hyperbranched fluorinated polymers offer better solutions. In particular, the latter has excellent transparency at telecommunication wavelengths, strong hydrophobicity, and long-term environmental and thermal stability.^[1,209,213,215,216,218]

A variety of other SWNT-based devices can be explored in future research. Aligned SWNTs could be used for birefringence filters and polarization rotating devices. Quantum-dot lasers could be mode-locked by integrating SWNT saturable absorbers directly into the dot laser cavity to achieve high repetition rates. SWNTs could be placed in index-matching gels, either in an external cavity or a trench. Microdisc and slab lasers could be fabricated with SWNT nonlinear elements. SWNT saturable absorbers could be placed into vertical-cavity surface emitting lasers. Ring lasers could be mode-locked in a hybrid way, by injection of the optical clocking signal into SWNTs (perpendicular to the lasing beam). Phase modulation mode-locking, using a similar scheme, but with wavelength off-resonance, could be explored. Multiple saturable absorbers could be used for harmonic mode-locking. Sol–gel structures could be fabricated with Er^{3+} and SWNT doping, to be applied as optical amplifiers and as compact waveguide lasers. A variety of active and passive devices with SWNTs composites could be fabricated for applications including, but not limited to, optical regeneration, pulse reshaping, dispersion compensation, pulse compression. SWNT have the potential to be used in optical gates (such as Mach–Zehnder interferometers) and ultrafast optical-sampling systems. Phase-conjugation devices could be realized for wave-front-aberrations and polarization-distortions removal. SWNT could be also placed in electro-optical modulators and micro cavities (Fabry–Perot). Photonic devices based on Franz–Keldysh/Stark effects could be realized. Optical waveguides could be engineered, incorporating nanotubes. The above devices could also be based on graphene.

The feasibility of SWNTs lasing (nanolasers based on CNTs as active medium) need also be investigated. Two-dimensional nanotube arrays could also be used for deep-UV photonic crystals and total visible absorbers.^[371]

Non-carbon nanomaterials can also be considered, for example, nanowires with promising optical properties, such as PbS, PbSe, CdSe, and Silicon.^[387,388] Boron Nitride nanotubes would be quite suitable for UV applications due to their large band gap.^[389]

In conclusion, nanotubes have enabled a new technology, specifically exploiting their electronic and optical properties,

which has improved the mode-locking performance of fiber lasers. These are key components in the photonic industry, but also have significant potential for deployment in applications such as laser cutting, welding, drilling, marking/engraving, microprocessing, surgery, and sensing, which serve a wide range of industries including automobile, aerospace, semiconductor, medical-device manufacturing, etc.

Acknowledgements

We acknowledge funding from EPSRC GR/S97613/01, EP/E500935/1, platform grant EP/F00897X/1, the European Research Council grant NANOPOTS, a Royal Society Brian Mercer Award for Innovation, British Council/Ministero dell' Università e della Ricerca, Isaac Newton Trust and Major State Basic Research Project No. G2009CB929300, China. This article is part of the Special Issue celebrating the 800th Anniversary of the University of Cambridge.

Received: April 2, 2009

Revised: June 16, 2009

- [1] H. Ma, A. K.-H. Jen, A. R. Dalton, *Adv. Mater.* **2002**, *14*, 1339.
- [2] L. R. Dalton, A. W. Harper, R. Ghosn, W. H. Steier, M. Ziari, H. Fetterman, Y. Shi, R. V. Mustacich, A. K. Y. Jen, K. J. Shea, *Chem. Mater.* **1995**, *7*, 1060.
- [3] R. Dersch, M. Steinhart, U. Boudriot, A. Greiner, J. H. Wendorff, *Polym. Adv. Technol.* **2005**, *16*, 276.
- [4] L. Dalton, A. Harper, A. Ren, F. Wang, G. Todorova, J. Chen, C. Zhang, M. Lee, *Ind. Eng. Chem. Res.* **1999**, *38*, 8.
- [5] L. Eldada, in *SPIE OE Mag.*, May **2002**, pp. 26–29.
- [6] L. Eldada, "Polymer microphotonics", presented at the *Conf. on Nano- and Micro-Optics for Information Systems*, San Diego, CA, August **2003**.
- [7] E. D. Lipp, A. L. Smith, in *The Analytical Chemistry of Silicones*, Vol. 112 (Ed: A. L. Smith), Wiley-Interscience, New York **1991**, p. 305.
- [8] H. J. Lee, M. H. Lee, S. G. Han, H. Y. Kim, J. H. Ahn, E. M. Lee, Y. H. Won, *J. Polym. Sci. Part A* **1998**, *36*, 301.
- [9] H. Ma, S. Liu, J. D. Luo, S. Suresh, L. Liu, S. H. Kang, M. Haller, T. Sassa, L. R. Dalton, A. K. Y. Jen, *Adv. Funct. Mater.* **2002**, *12*, 565.
- [10] R. J. Mears, L. Reekie, I. M. Jauncey, D. N. Payne, *Electron. Lett.* **1987**, *23*, 1026.
- [11] *Optical Amplifiers and Their Applications* (Eds: S. Shimada, H. Ishio), Wiley & Sons Ltd., New York **1992**.
- [12] H. Liang, Q. Zhang, Z. Zheng, H. Ming, Z. Li, J. Xu, B. Chen, H. Zhao, *Opt. Lett.* **2004**, *29*, 477.
- [13] W. H. Wong, E. Y. B. Pun, K. S. Chan, *Appl. Phys. Lett.* **2004**, *84*, 176.
- [14] L. H. Slooff, A. van Blaaderen, A. Polman, G. A. Hebbink, S. I. Klink, F. Van Veggel, D. N. Reinhoudt, J. W. Hofstra, *J. Appl. Phys.* **2002**, *91*, 3955.
- [15] R. Brinkmann, W. Sohler, H. Suche, *Electron. Lett.* **1991**, *27*, 415.
- [16] C. Koeppen, S. Yamada, G. Jiang, A. F. Garito, L. R. Dalton, *J. Opt. Soc. Am. B* **1997**, *14*, 155.
- [17] L. H. Slooff, A. Polman, M. P. O. Wolbers, F. C. J. M. v. Veggel, D. N. Reinhoudt, J. W. Hofstra, *J. Appl. Phys.* **1998**, *83*, 497.
- [18] M. A. Burns, B. N. Johnson, S. N. Brahmasandra, K. Handique, J. R. Webster, M. Krishnan, T. S. Sammarco, P. M. Man, D. Jones, D. Heldsinger, C. H. Mastrangelo, D. T. Burke, *Science* **1998**, *282*, 484.
- [19] G. Camino, S. M. Lomakin, M. Lazzari, *Polymer* **2001**, *42*, 2395.
- [20] J. Jon, V. DeGroot, A. Norris, S. O. Glover, T. V. Clapp, "Highly transparent silicone materials", presented at the *Linear and Nonlinear Optics of Organic Materials Conf. IV*, Denver, CO, August, **2004**.
- [21] G. P. Agrawal, *Nonlinear Fiber Optics*, Academic Press, San Diego **2001**.
- [22] *Nonlinear Optics in Semiconductors I* (Eds: R. K. Willardson, E. R. Weber, E. Garmire, A. Kost), Academic Press, San Diego, **1999**.
- [23] *Commercial and Biomedical Applications of Ultrafast Lasers* (Eds: M. K. Reed, J. Neev), SPIE, Bellingham, WA **1999**.
- [24] U. Keller, *Nature* **2003**, *424*, 831.
- [25] P. W. Smith, *Proc. IEEE* **1970**, *58*, 1342.
- [26] A. J. DeMaria, D. A. Stetser, H. Heynau, *Appl. Phys. Lett.* **1966**, *8*, 174.
- [27] H. W. Mocker, R. J. Collins, *Appl. Phys. Lett.* **1965**, *7*, 270.
- [28] N. Sarukura, Y. Ishida, T. Yanagawa, H. Nakano, *Appl. Phys. Lett.* **1990**, *57*, 229.
- [29] E. Giorgetti, G. Margheri, S. Sottini, M. Casalboni, R. Senesi, M. Scarselli, R. Pizzoferrato, *J. Non-Cryst. Solids* **1999**, *255*, 193.
- [30] W. Koechner, *Solid-State Laser Engineering*, Springer Science, Berlin **2006**.
- [31] G. Steinmeyer, D. H. Sutter, L. Gallmann, N. Matuschek, U. Keller, *Science* **1999**, *286*, 1507.
- [32] U. Keller, in *Progress in Optics*, Vol. 46 (Ed: E. Wolf), Elsevier, Amsterdam **2004**.
- [33] L. E. Adams, E. S. Kintzer, M. Ramaswamy, J. G. Fujimoto, U. Keller, M. T. Asom, *Opt. Lett.* **1993**, *18*, 1940.
- [34] A. Braun, J. V. Rudd, H. Cheng, G. Mourou, D. Kopf, I. D. Jung, K. J. Weingarten, U. Keller, *Opt. Lett.* **1995**, *20*, 1889.
- [35] M. E. Fermann, J. D. Minelly, *Opt. Lett.* **1996**, *21*, 970.
- [36] S. T. Cundiff, B. C. Collings, W. H. Knox, *Opt. Express* **1997**, *1*, 12.
- [37] D. Kopf, A. Prasad, G. Zhang, M. Moser, U. Keller, *Opt. Lett.* **1997**, *22*, 621.
- [38] D. N. Papadopoulos, S. Forget, M. Delaigue, F. Druon, F. Balembis, P. Georges, *Opt. Lett.* **2003**, *28*, 1838.
- [39] S. J. Holmgren, A. Fragemann, V. Pasiskevicius, F. Laurell, *Opt. Express* **2006**, *14*, 6675.
- [40] F. Hoos, S. Pricking, H. Giessen, *Opt. Express* **2006**, *14*, 10913.
- [41] S. V. Marchese, T. Sudmeyer, M. Golling, R. Grange, U. Keller, *Opt. Lett.* **2006**, *31*, 2728.
- [42] C. Lecaplain, C. Chedot, A. Hideur, B. Ortac, J. Limpert, *Opt. Lett.* **2007**, *32*, 2738.
- [43] B. Ortac, O. Schmidt, T. Schreiber, J. Limpert, A. Tunnermann, A. Hideur, *Opt. Express* **2007**, *15*, 10725.
- [44] E. Garmire, *IEEE J. Sel. Top. Quantum Electron.* **2000**, *6*, 1094.
- [45] O. Okhotnikov, A. Grudinin, M. Pessa, *New J. Phys.* **2004**, *6*, 177.
- [46] O. Wada, *New J. Phys.* **2004**, *6*, 183.
- [47] A. Isomaki, A. M. Vainionpaa, J. Lyytikainen, O. G. Okhotnikov, *IEEE J. Quantum Electron.* **2003**, *39*, 1481.
- [48] E. Burr, M. Pantouvaki, M. Fice, R. Gwilliam, A. Krysa, J. Roberts, A. Seeds, *J. Lightwave Technol.* **2006**, *24*, 747.
- [49] N. Xiang, M. D. Guina, A. M. Vainionpaa, J. Lyytikainen, S. Suomalainen, M. J. Saarinen, O. Okhotnikov, T. Sajaavaara, J. Keinonen, *IEEE J. Quantum Electron.* **2002**, *38*, 369.
- [50] F. J. Grawert, J. T. Gopinath, F. O. Ilday, H. M. Shen, E. P. Ippen, F. X. Kartner, S. Akiyama, J. Liu, K. Wada, L. C. Kimerling, *Opt. Lett.* **2005**, *30*, 329.
- [51] T. Y. Fan, G. Huber, R. L. Byer, P. Mitzscherlich, *IEEE J. Quantum Electron.* **1988**, *24*, 924.
- [52] L. Esterowitz, *Opt. Eng.* **1990**, *29*, 676.
- [53] S. W. Henderson, C. P. Hale, J. R. Magee, M. J. Kavaya, A. V. Huffaker, *Opt. Lett.* **1991**, *16*, 773.
- [54] K. Scholle, E. Heumann, G. Huber, *Laser Phys. Lett.* **2004**, *1*, 285.
- [55] G. J. Koch, B. W. Barnes, M. Petros, J. Y. Beyon, F. Amzajerdian, J. R. Yu, R. E. Davis, S. Ismail, S. Vay, M. J. Kavaya, U. N. Singh, *Appl. Opt.* **2004**, *43*, 5092.
- [56] M. R. Treat, S. L. Trokel, R. D. Reynolds, V. J. Defilippi, J. Andrew, J. Y. Liu, M. G. Cohen, *Laser Surg. Med.* **1988**, *8*, 322.
- [57] J. H. V. Price, T. M. Monro, H. Ebendorff Heidepriem, F. Poletti, V. Finazzi, J. Y. Y. Leong, P. Petropoulos, J. C. Flanagan, G. Brambilla, X. Feng, D. J. Richardson, in *SPIE, Fiber Lasers III: Technology, Systems, Applications* (Eds: A. J. W. Brown, J. Nilsson, D. J. Harter, A. Tunnerman), Vol. 6102, SPIE, Bellingham, WA **2006**.
- [58] V. D. Taranukhin, N. Y. Shubin, *J. Opt. Soc. Am. B* **2000**, *17*, 1509.
- [59] G. Mourou, D. Umstadter, *Sci. Am.* **2002**, *5*, 81.

- [60] R. C. Sharp, D. E. Spock, N. Pan, J. Elliot, *Opt. Lett.* **1996**, *21*, 881.
- [61] O. Jost, A. A. Gorbunov, W. Pompe, T. Pichler, R. Friedlein, M. Knupfer, M. Reibold, H. D. Bauer, L. Dunsch, M. S. Golden, J. Fink, *Appl. Phys. Lett.* **1999**, *75*, 2217.
- [62] M. J. O'Connell, S. M. Bachilo, C. B. Huffman, V. C. Moore, M. S. Strano, E. H. Haroz, K. L. Rialon, P. J. Boul, W. H. Noon, C. Kittrell, J. Ma, R. H. Hauge, R. B. Weisman, R. E. Smalley, *Science* **2002**, *297*, 593.
- [63] M. Zheng, A. Jagota, E. D. Semke, B. A. Diner, R. S. Mclean, S. R. Lustig, R. E. Richardson, N. G. Tassi, *Nat. Mater.* **2003**, *2*, 338.
- [64] M. Zheng, A. Jagota, M. S. Strano, A. P. Santos, P. Barone, S. G. Chou, B. A. Diner, M. S. Dresselhaus, R. S. McLean, G. B. Onoa, G. G. Samsonidze, E. D. Semke, M. Usrey, D. J. Walls, *Science* **2003**, *302*, 1545.
- [65] H. Kataura, Y. Kumazawa, Y. Maniwa, I. Umezu, S. Suzuki, Y. Ohtsuka, Y. Achiba, *Synth. Met.* **1999**, *103*, 2555.
- [66] S. M. Bachilo, M. S. Strano, C. Kittrell, R. H. Hauge, R. E. Smalley, R. B. Weisman, *Science* **2002**, *298*, 2361.
- [67] P. H. Tan, A. G. Rozhin, T. Hasan, P. Hu, V. Scardaci, W. I. Milne, A. C. Ferrari, *Phys. Rev. Lett.* **2007**, *99*, 137402.
- [68] P. H. Tan, T. Hasan, F. Bonaccorso, V. Scardaci, A. G. Rozhin, W. I. Milne, A. C. Ferrari, *Phys. E* **2008**, *40*, 2352.
- [69] S. Reich, C. Thomsen, J. Robertson, *Phys. Rev. Lett.* **2005**, *95*, 077402.
- [70] F. Wang, G. Dukovic, L. E. Brus, T. F. Heinz, *Science* **2005**, *308*, 838.
- [71] J. Maultzsch, R. Pomraenke, S. Reich, E. Chang, D. Prezzi, A. Ruini, E. Molinari, M. S. Strano, C. Thomsen, C. Lienau, *Phys. Rev. B* **2005**, *72*, 241402(R).
- [72] S. G. Chou, F. Plentz, J. Jiang, R. Saito, D. Nezich, H. B. Ribeiro, A. Jorio, M. A. Pimenta, G. G. Samsonidze, A. P. Santos, M. Zheng, G. B. Onoa, E. D. Semke, G. Dresselhaus, M. S. Dresselhaus, *Phys. Rev. Lett.* **2005**, *94*, 127402.
- [73] F. Plentz, H. B. Ribeiro, A. Jorio, M. S. Strano, M. A. Pimenta, *Phys. Rev. Lett.* **2005**, *95*, 247401.
- [74] Y. Miyauchi, S. Maruyama, *Phys. Rev. B* **2006**, *74*, 035415.
- [75] Y. Miyauchi, R. Saito, K. Sato, Y. Ohno, S. Iwasaki, T. Mizutani, J. Jiang, S. Maruyama, *Chem. Phys. Lett.* **2007**, *442*, 394.
- [76] J. Lefebvre, P. Finnie, *Phys. Rev. Lett.* **2007**, *98*, 167406.
- [77] O. Kiowski, K. Arnold, S. Lebedkin, F. Hennrich, M. M. Kappes, *Phys. Rev. Lett.* **2007**, *99*, 237402.
- [78] O. Kiowski, S. Lebedkin, F. Hennrich, M. M. Kappes, *Phys. Rev. B* **2007**, *76*, 075422.
- [79] S. Lebedkin, F. Hennrich, O. Kiowski, M. M. Kappes, *Phys. Rev. B* **2008**, *77*, 165429.
- [80] V. Perebeinos, J. Tersoff, P. Avouris, *Phys. Rev. Lett.* **2005**, *94*, 027402.
- [81] J. Lefebvre, P. Finnie, *Nano Lett.* **2008**, *8*, 1890.
- [82] T. Hertel, R. Fasel, G. Moos, *Appl. Phys. A* **2002**, *75*, 449.
- [83] Y.-C. Chen, N. R. Ravavikar, L. S. Schadler, P. M. Ajayan, Y.-P. Zhao, T.-M. Lu, G.-C. Wang, X.-C. Zhang, *Appl. Phys. Lett.* **2002**, *81*, 975.
- [84] S. Tatsuura, M. Furuki, Y. Sato, I. Iwasa, M. Tian, H. Mitsu, *Adv. Mater.* **2003**, *15*, 534.
- [85] J. S. Lauret, C. Voisin, G. Cassabois, C. Delalande, P. Roussignol, O. Jost, L. Capes, *Phys. Rev. Lett.* **2003**, *90*, 057404/1.
- [86] W. Feng, W. H. Yi, H. C. Wu, M. Ozaki, K. Yoshino, *J. Appl. Phys.* **2005**, *98*, 7.
- [87] V. A. Margulis, *J. Phys. Condens. Matter* **1999**, *11*, 3065.
- [88] V. A. Margulis, T. A. Sizikova, *Phys. B* **1998**, *245*, 173.
- [89] V. A. Margulis, E. A. Gaiduk, E. N. Zhidkin, *Diamond Relat. Mater.* **1999**, *8*, 1240.
- [90] S. Y. Set, H. Yaguchi, Y. Tanaka, M. Jablonski, *J. Lightwave Technol.* **2004**, *22*, 51.
- [91] K. Ramadurai, C. L. Cromer, L. A. Lewis, K. E. Hurst, A. C. Dillon, R. L. Mahajan, J. H. Lehman, *J. Appl. Phys.* **2008**, *103*, 013103.
- [92] C. L. Cromer, K. E. Hurst, X. Y. Li, J. H. Lehman, *Opt. Lett.* **2009**, *34*, 193.
- [93] S. Yamashita, S. Y. Set, C. S. Goh, K. Kikuchi, *Electron. Commun. Jpn. Part 2* **2007**, *90*, 17.
- [94] Y. Sakakibara, A. G. Rozhin, H. Kataura, Y. Achiba, H. Tokumoto, *Jpn. J. Appl. Phys. Part 1* **2005**, *44*, 1621.
- [95] G. Della Valle, R. Osellame, G. Galzerano, N. Chiodo, G. Cerullo, P. Laporta, O. Svelto, U. Morgner, A. G. Rozhin, V. Scardaci, A. C. Ferrari, *Appl. Phys. Lett.* **2006**, *89*, 231115.
- [96] V. Scardaci, Z. Sun, F. Wang, A. G. Rozhin, T. Hasan, F. Hennrich, I. H. White, W. I. Milne, A. C. Ferrari, *Adv. Mater.* **2008**, *20*, 4040.
- [97] Z. Sun, A. G. Rozhin, F. Wang, V. Scardaci, W. I. Milne, I. H. White, F. Hennrich, A. C. Ferrari, *Appl. Phys. Lett.* **2008**, *93*, 061114.
- [98] F. Wang, A. G. Rozhin, V. Scardaci, Z. Sun, F. Hennrich, I. H. White, W. I. Milne, A. C. Ferrari, *Nat. Nanotechnol.* **2008**, *3*, 738.
- [99] A. Martinez, S. Uchida, Y. W. Song, T. Ishigure, S. Yamashita, *Opt. Express* **2008**, *16*, 11337.
- [100] F. Shohda, T. Shirato, M. Nakazawa, K. Komatsu, T. Kaino, *Opt. Express* **2008**, *16*, 21191.
- [101] F. Shohda, T. Shirato, M. Nakazawa, J. Mata, J. Tsukamoto, *Opt. Express* **2008**, *16*, 20943.
- [102] M. Nakazawa, S. Nakahara, T. Hirooka, M. Yoshida, T. Kaino, K. Komatsu, *Opt. Lett.* **2006**, *31*, 915.
- [103] Y. Maeda, S.-i. Kimura, Y. Hirashima, M. Kanda, Y. Lian, T. Wakahara, T. Akasaka, T. Hasegawa, H. Tokumoto, T. Shimizu, H. Kataura, Y. Miyauchi, S. Maruyama, K. Kobayashi, S. Nagase, *J. Phys. Chem. B* **2004**, *108*, 18395.
- [104] S. Giordani, S. D. Bergin, V. Nicolosi, S. Lebedkin, M. M. Kappes, W. J. Blau, J. N. Coleman, *J. Phys. Chem. B* **2006**, *110*, 15708.
- [105] T. Hasan, P. H. Tan, F. Bonaccorso, A. Rozhin, V. Scardaci, W. I. Milne, A. C. Ferrari, *J. Phys. Chem. C* **2008**, *112*, 20227.
- [106] R. Haggenmueller, S. S. Rahatekar, J. A. Fagan, J. H. Chun, M. L. Becker, R. R. Naik, T. Krauss, L. Carlson, J. F. Kadla, P. C. Trulove, D. F. Fox, H. C. DeLong, Z. C. Fang, S. O. Kelley, J. W. Gilman, *Langmuir* **2008**, *24*, 5070.
- [107] H. Gu, T. M. Swager, *Adv. Mater.* **2008**, *20*, 1.
- [108] T. Kashiwagi, J. Fagan, J. Douglas, K. Yamamoto, A. Heckert, S. Leigh, J. Obrzut, F. Du, S. Lin-Gibson, M. Mu, K. Winey, R. Haggenmueller, *Polymer* **2007**, *48*, 4855.
- [109] J. Liu, T. Liu, S. Kumar, *Polymer* **2005**, *46*, 3419.
- [110] S. D. Bergin, V. Nicolosi, P. V. Streich, S. Giordani, Z. Sun, A. H. Windle, P. Ryan, N. P. P. Niraj, Z. T. Wang, L. Carpenter, W. J. Blau, J. J. Boland, J. P. Hamilton, J. N. Coleman, *Adv. Mater.* **2008**, *20*, 1876.
- [111] K. D. Ausman, R. Piner, O. Lourie, R. S. Ruoff, M. Korobov, *J. Phys. Chem. B* **2000**, *104*, 8911.
- [112] B. J. Landi, H. J. Ruf, J. J. Worman, R. P. Raffaele, *J. Phys. Chem. B* **2004**, *108*, 17089.
- [113] P. M. Ajayan, O. Stephan, C. Colliex, D. Trauth, *Science* **1994**, *265*, 1212.
- [114] J. N. Coleman, U. Khan, Y. K. Gun'ko, *Adv. Mater.* **2006**, *18*, 689.
- [115] A. B. Dalton, S. Collins, E. Muñoz, J. M. Razal, V. H. Ebron, J. P. Ferraris, J. N. Coleman, B. G. Kim, R. H. Baughman, *Nature* **2003**, *423*, 703.
- [116] R. H. Baughman, A. A. Zakhidov, W. A. de Heer, *Science* **2002**, *297*, 787.
- [117] A. B. Dalton, S. Collins, J. Razal, E. Munoz, V. H. Ebron, B. G. Kim, J. N. Coleman, J. P. Ferraris, R. H. Baughman, *J. Mater. Chem.* **2004**, *14*, 1.
- [118] M. Zhang, K. R. Atkinson, R. H. Baughman, *Science* **2004**, *306*, 1358.
- [119] S. Banerjee, T. Hemraj-Benny, S. S. Wong, *Adv. Mater.* **2005**, *17*, 17.
- [120] C. Park, Z. Ounaies, K. A. Watson, R. E. Crooks, J. Smith, S. E. Lowther, J. W. Connell, E. J. Siochi, J. S. Harrison, T. L. S. Clair, *Chem. Phys. Lett.* **2002**, *364*, 303.
- [121] K. W. Putz, C. A. Mitchell, R. Krishnamoorti, P. F. Green, *J. Polym. Sci. Part B* **2004**, *42*, 2286.
- [122] O. Breuer, U. Sundararaj, *Polym. Compos.* **2004**, *25*, 630.
- [123] S. V. Ahir, Y. Y. Huang, E. M. Terentjev, *Polymer* **2008**, *49*, 3841.
- [124] Y. Sakakibara, K. Kintaka, A. G. Rozhin, T. Itatani, W. M. Soe, H. Itatani, M. Tokumoto, H. Kataura, presented at the *31st European Conf. on Optical Communication*, Glasgow, Scotland, September 2005.
- [125] V. Scardaci, A. G. Rozhin, P. H. Tan, F. Wang, I. H. White, W. I. Milne, A. C. Ferrari, *Phys. Status Solidi B* **2007**, *244*, 4303.
- [126] S. Kazaoui, N. Minami, B. Nalini, Y. Kim, N. Takada, K. Hara, *Appl. Phys. Lett.* **2005**, *87*, 211914.
- [127] Z. Xu, Y. Wu, B. Hu, I. N. Ivanov, D. B. Geohegan, *Appl. Phys. Lett.* **2005**, *87*, 263118.

- [128] S. Kazaoui, N. Minami, B. Nalini, Y. Kim, K. Hara, *J. Appl. Phys.* **2005**, *98*, 084314.
- [129] H. Ago, K. Petrich, M. S. P. Shaffer, A. H. Windle, R. H. Friend, *Adv. Mater.* **1999**, *11*, 1281.
- [130] C. Li, Y. Chen, Y. Wang, Y. Wang, M. Chhowalla, S. Mitra, *J. Mater. Chem.* **2007**, *17*, 2406.
- [131] B. Pradhan, S. K. Batabyal, A. J. Pal, *Appl. Phys. Lett.* **2006**, *88*, 093106.
- [132] E. Kymakis, G. A. J. Amaratunga, *Appl. Phys. Lett.* **2002**, *80*, 112.
- [133] E. Kymakis, I. Alexandrou, G. A. J. Amaratunga, *J. Appl. Phys.* **2003**, *93*, 1764.
- [134] E. Kymakis, G. A. J. Amaratunga, *Sol. Energy Mater. Sol. Cells* **2003**, *80*, 465.
- [135] A. A. Green, M. C. Hersam, *Nano Lett.* **2008**, *8*, 1417.
- [136] B. B. Parekh, G. Fanchini, G. Eda, M. Chhowalla, *Appl. Phys. Lett.* **2007**, *90*, 3.
- [137] M. Chhowalla, *J. Soc. Inf. Disp.* **2007**, *15*, 1085.
- [138] A. Heras, A. Colina, J. López-Palacios, A. Kaskela, A. G. Nasibulin, V. Ruiz, E. I. Kauppinen, *Electrochem. Commun.* **2009**, *11*, 442.
- [139] S. De, P. E. Lyons, S. Sorel, E. M. Doherty, P. J. King, W. J. Blau, P. N. Nirmalraj, J. J. Boland, V. Scardaci, J. Joimel, J. N. Coleman, *ACS Nano* **2009**, *3*, 714.
- [140] Z. Wu, Z. Chen, X. Du, J. M. Logan, J. Sippel, M. Nikolou, K. Kamaras, J. R. Reynolds, D. B. Tanner, A. F. Hebard, A. G. Rinzler, *Science* **2004**, *305*, 1273.
- [141] G. Gruner, *J. Mater. Chem.* **2006**, *16*, 3533.
- [142] U. Dettlaff-Weglikowska, M. Kaempgen, B. Hornbostel, V. Skakalova, J. Wang, J. Liang, S. Roth, *Phys. Status Solidi B* **2006**, *243*, 3440.
- [143] D. Zhang, K. Ryu, X. Liu, E. Polikarpov, J. Ly, M. E. Tompson, C. Zhou, *Nano Lett.* **2006**, *6*, 1880.
- [144] N. Ferrer-Anglada, M. Kaempgen, V. Skakalova, U. Dettlaff-Weglikowska, S. Roth, *Diamond Relat. Mater.* **2004**, *13*, 256.
- [145] S. Y. Set, H. Yaguchi, Y. Tanaka, M. Jablonski, *IEEE J. Sel. Top. Quantum Electron.* **2004**, *10*, 137.
- [146] K. Kieu, M. Mansuripur, *Opt. Lett.* **2007**, *32*, 2242.
- [147] A. G. Rozhin, V. Scardaci, F. Wang, F. Hennrich, I. H. White, W. I. Milne, A. C. Ferrari, *Phys. Status Solidi B* **2006**, *243*, 3551.
- [148] A. G. Rozhin, Y. Sakakibara, S. Namiki, M. Tokumoto, H. Kataura, *Appl. Phys. Lett.* **2006**, *88*, 051118.
- [149] K. H. Fong, K. Kikuchi, C. H. Goh, S. Y. Set, R. Grange, M. Haiml, A. Schlatter, U. Keller, *Opt. Lett.* **2007**, *32*, 38.
- [150] T. R. Schibli, K. Minoshima, H. Kataura, E. Itoga, N. Minami, S. Kazaoui, K. Miyashita, M. Tokumoto, Y. Sakakibara, *Opt. Express* **2005**, *13*, 8025.
- [151] S. Yamashita, Y. Inoue, H. Yaguchi, M. Jablonski, S. Y. Set, "S-, C-, L-Band Picosecond Fiber Pulse Sources Using a Broadband Carbon-Nanotube-based Mode-Locker" presented at the *European Conf. on Opt. Comm. (ECOC)*, Stockholm, Sweden, September **2004**.
- [152] M. A. Solodyankin, E. D. Obraztsova, A. S. Lobach, A. I. Chernov, A. V. Tausenev, V. I. Konov, E. M. Dianov, *Opt. Lett.* **2008**, *33*, 1336.
- [153] A. V. Tausenev, E. D. Obraztsova, A. S. Lobach, A. I. Chernov, V. I. Konov, P. G. Kryukov, A. V. Konyashchenko, E. M. Dianov, *Appl. Phys. Lett.* **2008**, *92*, 171113.
- [154] Y. W. Song, K. Morimune, S. Y. Set, S. Yamashita, *Appl. Phys. Lett.* **2007**, *90*, 021101.
- [155] Y. W. Song, S. Yamashita, C. S. Goh, S. Y. Set, *Opt. Lett.* **2007**, *32*, 430.
- [156] F. Wang, A. G. Rozhin, Z. Sun, V. Scardaci, I. H. White, A. C. Ferrari, *Phys. Status Solidi B* **2008**, *245*, 2319.
- [157] E. J. R. Kelleher, J. C. Travers, Z. Sun, A. Rozhin, A. C. Ferrari, S. V. Popov, J. R. Taylor, *Appl. Phys. Lett.* **2009**, *95*, 111108.
- [158] Z. Sun, A. G. Rozhin, F. Wang, T. Hasan, D. Popa, V. Scardaci, A. C. Ferrari, unpublished.
- [159] Z. Sun, A. G. Rozhin, F. Wang, V. Scardaci, I. H. White, A. C. Ferrari, unpublished.
- [160] J. Mangeney, S. Barre, G. Aubin, J. L. Oudar, O. Leclerc, *Electron. Lett.* **2000**, *36*, 1725.
- [161] K. K. Chow, S. Yamashita, Y. W. Song, *Opt. Express* **2009**, *17*, 7664.
- [162] S. A. O'Flaherty, R. Murphy, S. V. Hold, M. Cadec, J. N. Coleman, W. J. Blau, *J. Phys. Chem. B* **2003**, *107*, 958.
- [163] G. de la Torre, P. Vazquez, F. Agullo-Lopez, T. Torres, *Chem. Rev.* **2004**, *104*, 3723.
- [164] W. Blau, H. Byrne, W. M. Dennis, J. M. Kelly, *Opt. Commun.* **1985**, *56*, 25.
- [165] F. Henari, J. Callaghan, H. Stiel, W. Blau, D. J. Cardin, *Chem. Phys. Lett.* **1992**, *199*, 144.
- [166] J. Callaghan, W. J. Blau, F. Z. Henari, *J. Nonlinear Opt. Phys. Mater.* **2000**, *9*, 505.
- [167] J. Wang, W. J. Blau, *Appl. Phys. B* **2008**, *91*, 521.
- [168] L. Vivien, E. Anglaret, D. Riehl, F. Bacou, C. Journet, C. Goze, M. Andrieux, M. Brunet, F. Lafonta, P. Bernier, F. Hache, *Chem. Phys. Lett.* **1999**, *307*, 317.
- [169] L. Vivien, E. Anglaret, D. Riehl, F. Hache, F. Bacou, M. Andrieux, F. Lafonta, C. Journet, C. Goze, M. Brunet, P. Bernier, *Opt. Commun.* **2000**, *174*, 271.
- [170] L. Vivien, P. Lancon, D. Riehl, F. Hache, E. Anglaret, *Carbon* **2002**, *40*, 1789.
- [171] Y. Chen, Y. Lin, Y. Liu, J. Doyle, N. He, X. Zhuang, J. Bai, W. J. Blau, *J. Nanosci. Nanotechnol.* **2007**, *7*, 1268.
- [172] R. W. Boyd, *Nonlinear Optics*, Academic, San Diego, CA **2003**.
- [173] W. T. Silfvast, *Laser Fundamentals*, Cambridge University Press, Cambridge **2004**.
- [174] O. Svelto, *Principles of Lasers*, Springer, New York **1998**.
- [175] C. F. Bohren, D. R. Huffman, *Absorption and Scattering of Light by Small Particles*, Wiley-Interscience, New York **1998**.
- [176] R. N. Zitter, *Appl. Phys. Lett.* **1969**, *14*, 73.
- [177] T. Akiyama, N. Georgiev, T. Mozume, H. Yoshida, A. V. Gopal, O. Wada, *Electron. Lett.* **2001**, *37*, 129.
- [178] H. I. Elim, W. Ji, M.-T. Ng, J. V. Vittal, *Appl. Phys. Lett.* **2007**, *90*, 033106.
- [179] H. I. Elim, J. Yang, J.-Y. Lee, J. Mi, W. Ji, *Appl. Phys. Lett.* **2006**, *88*, 083107.
- [180] V. G. Savitski, A. M. Malyarevich, M. I. Demchuk, K. V. Yumashev, H. Raaben, A. A. Zhilin, *J. Opt. Soc. Am. B* **2005**, *22*, 1660.
- [181] Y. V. Vandyshev, V. S. Dneprovskii, V. I. Klimov, *Sov. Phys. JETP* **1992**, *74*, 144.
- [182] S. Y. Set, H. Yaguchi, Y. Tanaka, M. Jablonski, Y. Sakakibara, A. Rozhin, M. Tokumoto, H. Kataura, Y. Achiba, K. Kikuchi, "Mode-locked Fiber Lasers based on a Saturable Absorber Incorporating Carbon Nanotubes", presented at the *Optical Fiber Communication Conf. (OFC)*, Washington, DC, March **2003**.
- [183] N. N. Il'ichev, S. V. Garnov, E. D. Obraztsova, *AIP Conf. Proc. Electronic Properties Novel Nanostructures* **2005**, *786*, 611.
- [184] S. Yamashita, Y. Inoue, S. Maruyama, Y. Murakami, H. Yaguchi, M. Jablonski, S. Y. Set, *Opt. Lett.* **2004**, *29*, 1581.
- [185] A. G. Rozhin, Y. Sakakibara, M. Tokumoto, H. Kataura, Y. Achiba, *Thin Solid Films* **2004**, *464-465*, 368.
- [186] V. Scardaci, A. G. Rozhin, F. Hennrich, W. I. Milne, A. C. Ferrari, *Phys. E* **2007**, *37*, 115.
- [187] Z. Sun, A. G. Rozhin, F. Wang, W. I. Milne, R. V. Pentyl, I. H. White, A. C. Ferrari, presented at the *Conf. on Lasers and Electro-Optics (CLEO)*, Baltimore, MD, May **2009**.
- [188] A. Gambetta, G. Galzerano, A. G. Rozhin, A. C. Ferrari, R. Ramponi, P. Laporta, M. Marangoni, *Opt. Express* **2008**, *16*, 11727.
- [189] S. V. Garnov, S. A. Solokhin, E. D. Obraztsova, A. S. Lobach, P. A. Obraztsov, A. L. Chernov, V. V. Bukin, A. A. Sirotkin, Y. D. Zagumennyi, Y. D. Zavartsev, S. A. Kutovoi, I. A. Shcherbakov, *Laser Phys. Lett.* **2007**, *4*, 648.
- [190] A. V. Tausenev, E. D. Obraztsova, A. S. Lobach, A. I. Chernov, V. I. Konov, A. V. Konyashchenko, P. G. Kryukov, E. M. Dianov, *Quantum Electron.* **2007**, *37*, 205.
- [191] K. Kieu, F. W. Wise, *Opt. Express* **2008**, *16*, 11453.
- [192] L. A. Girifalco, M. Hodak, R. S. Lee, *Phys. Rev. B* **2000**, *62*, 13104.
- [193] G. Mie, *Ann. Phys.* **1908**, *330*, 377.
- [194] A. G. Rozhin, Y. Sakakibara, H. Kataura, S. Matsuzaki, K. Ishida, Y. Achiba, M. Tokumoto, *Chem. Phys. Lett.* **2005**, *405*, 288.

- [195] V. C. Moore, M. S. Strano, E. H. Haroz, R. H. Hauge, R. E. Smalley, *Nano Lett.* **2003**, *3*, 1379.
- [196] F. Bonaccorso, T. Hasan, P. H. Tan, A. G. Rozhin, G. Di Marco, P. G. Gucciardi, A. C. Ferrari, unpublished.
- [197] T. Hasan, V. Scardaci, P. H. Tan, A. G. Rozhin, W. I. Milne, A. C. Ferrari, *J. Phys. Chem. C* **2007**, *111*, 12594.
- [198] T. Hasan, V. Scardaci, P. H. Tan, A. G. Rozhin, W. I. Milne, A. C. Ferrari, *Phys. E* **2008**, *40*, 2414.
- [199] R. Bandyopadhyaya, E. Nativ-Roth, O. Regev, R. Yerushalmi-Rozen, *Nano Lett.* **2002**, *2*, 25.
- [200] M. J. O'Connell, P. Boul, L. M. Ericson, C. Huffman, Y. Wang, E. Haroz, C. Kuper, J. Tour, K. D. Ausman, R. E. Smalley, *Chem. Phys. Lett.* **2001**, *342*, 265.
- [201] N. Minami, Y. Kim, K. Miyashita, S. Kazaoui, B. Nalini, *Appl. Phys. Lett.* **2006**, *88*, 093123.
- [202] Y. Sakakibara, S. Tatsuura, H. Kataura, M. Tokumoto, Y. Achiba, *Jpn. J. Appl. Phys. Part 2* **2003**, *42*, L494.
- [203] D. E. Resasco, W. E. Alvarez, F. Pompeo, L. Balzano, J. E. Herrera, B. Kitiyanan, A. Borgna, *J. Nanopart. Res.* **2002**, *4*, 131.
- [204] S. Lebedkin, P. Schweiss, B. Renker, S. Malik, F. Hennrich, M. Neumaier, C. Stoermer, M. M. Kappes, *Carbon* **2002**, *40*, 417.
- [205] P. Nikolaev, M. J. Bronikowski, R. K. Bradley, F. Rohmund, D. T. Colbert, K. A. Smith, R. E. Smalley, *Chem. Phys. Lett.* **1999**, *313*, 91.
- [206] H. Kataura, Y. Kumazawa, Y. Maniwa, Y. Ohtsuka, R. Sen, S. Suzuki, Y. Achiba, *Carbon* **2000**, *38*, 1691.
- [207] S. Kivistö, T. Hakulinen, A. Kaskela, B. Aitchison, D. P. Brown, A. G. Nasibulin, E. I. Kauppinen, A. Härkönen, O. G. Okhotnikov, *Opt. Express* **2009**, *17*, 2358.
- [208] A. Skumanich, C. R. Moylan, *Chem. Phys. Lett.* **1990**, *174*, 139.
- [209] S. H. Kang, J. D. Luo, H. Ma, R. R. Barto, C. W. Frank, L. R. Dalton, A. K. Y. Jen, *Macromolecules* **2003**, *36*, 4355.
- [210] M. Kagami, H. Ito, T. Ichikawa, S. Kato, M. Matsuda, N. Takahashi, *Appl. Opt.* **1995**, *34*, 1041.
- [211] S. Singh, A. Kapoor, S. C. K. Misra, K. N. Tripathi, *Solid State Commun.* **1996**, *100*, 503.
- [212] M. Hikita, R. Yoshimura, M. Usui, S. Tomaru, S. Imamura, *Thin Solid Films* **1997**, *331*, 303.
- [213] T. Matsuura, J. Kobayashi, S. Ando, T. Maruno, S. Sasaki, F. Yamamoto, *Appl. Opt.* **1999**, *38*, 966.
- [214] L. Eldada, L. W. Shacklette, *IEEE J. Sel. Top. Quantum Electron.* **2000**, *6*, 54.
- [215] B. L. Booth, *J. Lightwave Technol.* **1989**, *7*, 1445.
- [216] R. Yoshimura, M. Hikita, S. Tomaru, S. Imamura, *J. Lightwave Technol.* **1998**, *16*, 1030.
- [217] S. Imamura, R. Yoshimura, T. Izawa, *Electron. Lett.* **1991**, *27*, 1342.
- [218] T. Matsuura, S. Ando, S. Sasaki, F. Yamamoto, *Electron. Lett.* **1993**, *29*, 269.
- [219] T. J. Mason, J. P. Lorimer, *Applied Sonochemistry: Uses of Power Ultrasound in Chemistry and Processing*, Wiley-VCH, Weinheim **2002**.
- [220] P. R. Birkin, D. G. Offen, P. F. Joseph, T. G. Leighton, *J. Phys. Chem. B* **2005**, *109*, 16997.
- [221] P. R. Birkin, T. G. Leighton, J. F. Power, M. D. Simpson, A. M. L. Vincotte, P. F. Joseph, *J. Phys. Chem. A* **2003**, *107*, 306.
- [222] P. R. Birkin, D. G. Offen, T. G. Leighton, *Phys. Chem. Chem. Phys.* **2005**, *7*, 530.
- [223] T. Hasan, Z. Sun, D. Popa, F. Wang, F. Bonaccorso, A. Rozhin, A. C. Ferrari, unpublished.
- [224] A. Hirsch, *Angew. Chem. Int. Ed.* **2002**, *41*, 1853.
- [225] J. L. Bahr, J. Yang, D. V. Kosynkin, M. J. Bronikowski, R. E. Smalley, J. M. Tour, *J. Am. Chem. Soc.* **2001**, *123*, 6536.
- [226] P. J. Boul, J. Liu, E. T. Mickelson, C. B. Huffman, L. M. Ericson, I. W. Chiang, K. A. Smith, D. T. Colbert, R. H. Hauge, J. L. Margrave, R. E. Smalley, *Chem. Phys. Lett.* **1999**, *310*, 367.
- [227] A. Garg, S. B. Sinnott, *Chem. Phys. Lett.* **1998**, *295*, 273.
- [228] J. L. Bahr, J. M. Tour, *J. Mater. Chem.* **2002**, *12*, 1952.
- [229] C. A. Dyke, J. M. Tour, *J. Am. Chem. Soc.* **2003**, *125*, 1156.
- [230] M. S. Strano, C. A. Dyke, M. L. Usrey, P. W. Barone, M. J. Allen, H. Shan, C. Kittrell, R. H. Hauge, J. M. Tour, R. E. Smalley, *Science* **2003**, *301*, 1519.
- [231] G. R. Dieckmann, A. B. Dalton, P. A. Johnson, J. Razal, J. Chen, G. M. Giordano, E. Munoz, I. H. Musselman, R. H. Baughman, R. K. Draper, *J. Am. Chem. Soc.* **2003**, *125*, 1770.
- [232] V. Zorbas, A. Ortiz-Acevedo, A. B. Dalton, M. M. Yoshida, G. R. Dieckmann, R. K. Draper, R. H. Baughman, M. Jose-Yacama, I. H. Musselman, *J. Am. Chem. Soc.* **2004**, *126*, 7222.
- [233] H. Xie, A. Ortiz-Acevedo, V. Zorbas, R. H. Baughman, R. K. Draper, I. H. Musselman, A. B. Dalton, G. R. Dieckmann, *J. Mater. Chem.* **2005**, *15*, 1734.
- [234] T. Takahashi, K. Tsunoda, H. Yajima, T. Ishii, *Jpn. J. Appl. Phys. Part 2* **2004**, *43*, 3636.
- [235] D. A. Britz, A. N. Khlobystov, *Chem. Soc. Rev.* **2006**, *35*, 637.
- [236] T. Umeyama, N. Kadota, N. Tezuka, Y. Matano, H. Imahori, *Chem. Phys. Lett.* **2007**, *444*, 263.
- [237] A. Star, J. F. Stoddart, D. Steuerman, M. Diehl, A. Boukai, E. W. Wong, X. Yang, S.-W. Chung, H. Choi, J. R. Heath, *Angew. Chem. Int. Ed.* **2001**, *40*, 1721.
- [238] A. Star, J. F. Stoddart, *Macromolecules* **2002**, *35*, 7516.
- [239] D. W. Steuerman, A. Star, R. Narizzano, H. Choi, R. S. Ries, C. Nicolini, J. F. Stoddart, J. R. Heath, *J. Phys. Chem. B* **2002**, *106*, 3124.
- [240] A. Star, Y. Liu, K. Grant, L. Ridvan, J. F. Stoddart, D. W. Steuerman, M. R. Diehl, A. Boukai, J. R. Heath, *Macromolecules* **2003**, *36*, 553.
- [241] M. F. Islam, E. Rojas, D. M. Bergey, A. T. Johnson, A. G. Yodh, *Nano Lett.* **2003**, *3*, 269.
- [242] S. K. Doorn, M. S. Strano, M. J. O'Connell, E. H. Haroz, K. L. Rialon, R. H. Hauge, R. E. Smalley, *J. Phys. Chem. B* **2003**, *107*, 6063.
- [243] H. Cathcart, S. Quinn, V. Nicolosi, J. M. Kelly, W. J. Blau, J. N. Coleman, *J. Phys. Chem. C* **2007**, *111*, 66.
- [244] M. S. Strano, M. Zheng, A. Jagota, G. B. Onoa, D. A. Heller, P. W. Barone, M. L. Usrey, *Nano Lett.* **2004**, *4*, 543.
- [245] T. Takahashi, C. R. Luculescu, K. Uchida, T. Ishii, H. Yajima, *Chem. Lett.* **2005**, *34*, 1516.
- [246] H. Butt, K. Graf, M. Kappl, *Physics and Chemistry of Interfaces*, 2nd ed. Wiley-VCH, Berlin **2006**.
- [247] W. Wenseleers, I. I. Vlasov, E. Goovaerts, E. D. Obratsova, A. S. Lobach, A. Bouwen, *Adv. Funct. Mater.* **2004**, *14*, 1105.
- [248] W. C. Herndon, *J. Chem. Educ.* **1967**, *44*, 724.
- [249] L. Picton, I. Bataille, G. Muller, *Carbohydr. Polym.* **2000**, *42*, 23.
- [250] J. Klein, P. Luckham, *Nature* **1982**, *300*, 429.
- [251] M. S. Arnold, S. I. Stupp, M. C. Hersam, *Nano Lett.* **2005**, *5*, 713.
- [252] Y. Noguchi, T. Fujigaya, Y. Niidome, N. Nakashima, *Chem. Phys. Lett.* **2008**, *455*, 249.
- [253] Y. Asada, H. Dohi, S. Kuwahara, T. Sugai, R. Kitaura, H. Shinohara, *Nano* **2007**, *2*, 295.
- [254] S. Malik, S. Vogel, H. Rosner, K. Arnold, F. Hennrich, A. K. Kohler, C. Richert, M. M. Kappes, *Compos. Sci. Technol.* **2007**, *67*, 916.
- [255] J. L. Bahr, E. T. Mickelson, M. J. Bronikowski, R. E. Smalley, J. M. Tour, *Chem. Commun.* **2001**, 193.
- [256] R. Krupke, F. Hennrich, O. Hampe, M. M. Kappes, *J. Phys. Chem. B* **2003**, *107*, 5667.
- [257] A. S. Labban, Y. Marcus, *J. Chem. Soc. Faraday Trans.* **1997**, *93*, 77.
- [258] J. A. Riddik, W. B. Bunger, T. K. Sakano, *Organic Solvents, Physical Properties and Methods of Purification*, Wiley, New York **1986**.
- [259] R. J. Chen, S. Bangsaruntip, K. A. Drouvalakis, N. W. S. Kam, M. Shim, Y. M. Li, W. Kim, P. J. Utz, H. J. Dai, *Proc. Natl. Acad. Sci. USA* **2003**, *100*, 4984.
- [260] A. Ikeda, K. Nobusawa, T. Hamano, J. Kikuchi, *Org. Lett.* **2006**, *8*, 5489.
- [261] Y. Kang, T. A. Taton, *J. Am. Chem. Soc.* **2003**, *125*, 5650.
- [262] A. Nish, J.-Y. Hwang, J. Doig, R. J. Nicholas, *Nat. Nanotechnol.* **2007**, *2*, 640.
- [263] S. Niyogi, S. Boukhalfa, S. B. Chikkannavar, T. J. McDonald, M. J. Heben, S. K. Doorn, *J. Am. Chem. Soc.* **2007**, *129*, 1898.

- [264] T. Rodgers, S. Shoji, Z. Sekkat, S. Kawata, *Phys. Rev. Lett.* **2008**, *101*, 127402.
- [265] H. P. Li, B. Zhou, Y. Lin, L. R. Gu, W. Wang, K. A. S. Fernando, S. Kumar, L. F. Allard, Y. P. Sun, *J. Am. Chem. Soc.* **2004**, *126*, 1014.
- [266] T. J. McDonald, J. L. Blackburn, W. K. Metzger, G. Rumbles, M. J. Heben, *J. Phys. Chem. C* **2007**, *111*, 17894.
- [267] M. S. Arnold, A. A. Green, J. F. Hulvat, S. I. Stupp, M. C. Hersam, *Nat. Nanotechnol.* **2006**, *1*, 60.
- [268] P. H. Tan, F. Bonaccorso, T. Hasan, V. Scardaci, A. Rozhin, P. G. Gucciardi, W. I. Milne, A. C. Ferrari, unpublished.
- [269] R. B. Weisman, S. M. Bachilo, *Nano Lett.* **2003**, *3*, 1235.
- [270] M. J. O'Connell, S. Sivaram, S. K. Doorn, *Phys. Rev. B* **2004**, *69*, 235415.
- [271] F. Wang, M. Y. Sfeir, L. Huang, X. M. H. Huang, Y. Wu, J. Kim, J. Hone, S. O'Brien, L. E. Brus, T. F. Heinz, *Phys. Rev. Lett.* **2006**, *96*, 167401.
- [272] A. G. Walsh, A. N. Vamvakas, Y. Yin, M. S. Ünlü, B. B. Goldberg, A. K. Swan, S. B. Cronin, *Nano Lett.* **2007**, *7*, 1485.
- [273] S. Reich, C. Thomsen, P. Ordejón, *Phys. Rev. B* **2002**, *65*, 155411.
- [274] S. M. Bachilo, L. Balzano, J. E. Herrera, F. Pompeo, D. E. Resasco, R. B. Weisman, *J. Am. Chem. Soc.* **2003**, *125*, 11186.
- [275] O. N. Torrens, M. Zheng, J. M. Kikkawa, *Phys. Rev. Lett.* **2008**, *101*, 4.
- [276] www.diagenode.com.
- [277] S. Takka, *Il Farmaco* **2003**, *58*, 1051.
- [278] C. Fantini, A. Jorio, M. Souza, M. S. Strano, M. S. Dresselhaus, M. A. Pimenta, *Phys. Rev. Lett.* **2004**, *93*, 147406.
- [279] J. Wu, W. Walukiewicz, W. Shan, E. Bourret-Courchesne, J. W. Ager III, K. M. Yu, E. E. Haller, K. Kissell, S. M. Bachilo, R. B. Weisman, R. E. Smalley, *Phys. Rev. Lett.* **2004**, *93*, 017404.
- [280] Y. Kim, N. Minami, S. Kazaoui, *Appl. Phys. Lett.* **2005**, *86*, 073103.
- [281] M. Lazzeri, S. Piscanec, F. Mauri, A. C. Ferrari, J. Robertson, *Phys. Rev. B* **2006**, *73*, 155426.
- [282] S. Piscanec, M. Lazzeri, J. Robertson, A. C. Ferrari, F. Mauri, *Phys. Rev. B* **2007**, *75*, 035427.
- [283] A. C. Ferrari, J. C. Meyer, V. Scardaci, C. Casiraghi, M. Lazzeri, F. Mauri, S. Piscanec, D. Jiang, K. S. Novoselov, S. Roth, A. K. Geim, *Phys. Rev. Lett.* **2006**, *97*, 187401.
- [284] T. M. G. Mohiuddin, A. Lombardo, R. R. Nair, A. Bonetti, G. Savini, R. Jalil, N. Bonini, D. M. Basko, C. Galiotis, N. Marzari, K. S. Novoselov, A. K. Geim, A. C. Ferrari, *Phys. Rev. B* **2009**, *79*, 205433.
- [285] P. T. Araujo, S. K. Doorn, S. Kilina, S. Tretiak, E. Einarsson, S. Maruyama, H. Chacham, M. A. Pimenta, A. Jorio, *Phys. Rev. Lett.* **2007**, *98*, 067401.
- [286] A. M. Rao, E. Richter, S. Bandow, B. Chase, P. C. Eklund, K. A. Williams, S. Fang, K. R. Subbaswamy, M. Menon, A. Thess, R. E. Smalley, G. Dresselhaus, M. S. Dresselhaus, *Science* **1997**, *275*, 187.
- [287] S. Bandow, S. Asaka, Y. Saito, A. M. Rao, L. Grigorian, E. Richter, P. C. Eklund, *Phys. Rev. Lett.* **1998**, *80*, 3779.
- [288] H. Telg, J. Maultzsch, S. Reich, F. Hennrich, C. Thomsen, *Phys. Rev. Lett.* **2004**, *93*, 177401.
- [289] J. C. Meyer, M. Paillet, T. Michel, A. Moreac, A. Neumann, G. S. Duesberg, S. Roth, J. L. Sauvajol, *Phys. Rev. Lett.* **2005**, *95*, 4.
- [290] R. A. Jishi, L. Venkataraman, M. S. Dresselhaus, G. Dresselhaus, *Chem. Phys. Lett.* **1993**, *209*, 77.
- [291] J. Kurti, G. Kresse, H. Kuzmany, *Phys. Rev. B* **1998**, *58*, R8869.
- [292] A. Jorio, R. Saito, J. H. Hafner, C. M. Lieber, M. Hunter, T. McClure, G. Dresselhaus, M. S. Dresselhaus, *Phys. Rev. Lett.* **2001**, *86*, 1118.
- [293] L. Alvarez, A. Righi, S. Rols, E. Anglaret, J. L. Sauvajol, E. Munoz, W. K. Maser, A. M. Benito, M. T. Martinez, G. F. de la Fuente, *Phys. Rev. B* **2001**, *63*, 153401.
- [294] V. N. Popov, V. E. Van Doren, M. Balkanski, *Phys. Rev. B* **1999**, *59*, 8355.
- [295] L. Henrard, E. Hernandez, P. Bernier, A. Rubio, *Phys. Rev. B* **1999**, *60*, R8521.
- [296] J. Maultzsch, H. Telg, S. Reich, C. Thomsen, *Phys. Rev. B* **2005**, *72*, 205438.
- [297] M. Paillet, T. Michel, J. C. Meyer, V. N. Popov, L. Henrard, S. Roth, J. L. Sauvajol, *Phys. Rev. Lett.* **2006**, *96*, 257401.
- [298] M. A. Pimenta, A. Marucci, S. A. Empedocles, M. G. Bawendi, E. B. Hanlon, A. M. Rao, P. C. Eklund, R. E. Smalley, G. Dresselhaus, M. S. Dresselhaus, *Phys. Rev. B* **1998**, *58*, 16016.
- [299] A. C. Ferrari, J. Robertson, *Phys. Rev. B* **2000**, *61*, 14095.
- [300] A. C. Ferrari, J. Robertson, *Phys. Rev. B* **2001**, *64*, 075414.
- [301] A. C. Ferrari, *Solid State Commun.* **2007**, *143*, 47.
- [302] S. Lebedkin, K. Arnold, F. Hennrich, R. Krupke, B. Renker, M. Kappes, *New J. Phys.* **2003**, *5*, 140.
- [303] O. J. Korovyanko, C. X. Sheng, Z. V. Vardeny, A. B. Dalton, R. H. Baughman, *Phys. Rev. Lett.* **2004**, *92*, 4.
- [304] U. Keller, K. J. Weingarten, F. X. Kärtner, D. Kopf, B. Braun, I. D. Jung, R. Fluck, C. Hönniger, N. Matuschek, J. Aus der Au, *IEEE J. Sel. Top. Quantum Electron.* **1996**, *2*, 435.
- [305] G. N. Ostojic, S. Zaric, J. Kono, M. S. Strano, V. C. Moore, R. H. Hauge, R. E. Smalley, *Phys. Rev. Lett.* **2004**, *92*, 117402.
- [306] G. Galzerano, M. Marano, S. Longhi, E. Sani, A. Toncelli, M. Tonelli, P. Laporta, *Opt. Lett.* **2003**, *28*, 2085.
- [307] E. W. Van Stryland, M. Sheik-Bahae, in *Characterization Techniques and Tabulations for Organic Nonlinear Optical Materials* (Eds: M. G. Kuzyk, C. W. Dirk), Marcel Dekker, New York **1998**.
- [308] M. Sheik-Bahae, A. A. Said, E. W. Van Stryland, *Opt. Lett.* **1989**, *14*, 955.
- [309] M. Sheik-Bahae, A. A. Said, T. H. Wei, D. J. Hagan, E. W. Van Stryland, *IEEE J. Quantum Electron.* **1990**, *26*, 760.
- [310] D. Shimamoto, T. Sakurai, M. Itoh, Y. A. Kim, T. Hayashi, M. Endo, M. Terrones, *Appl. Phys. Lett.* **2008**, *92*, 081902.
- [311] W. B. Cho, J. H. Yim, S. Y. Choi, S. Lee, U. Griebner, V. Petrov, F. Rotermund, *Opt. Lett.* **2008**, *33*, 2449.
- [312] A. Schmidt, S. Rivier, G. Steinmeyer, J. H. Yim, W. B. Cho, S. Lee, F. Rotermund, M. C. Pujol, X. Mateos, M. Aguilo, F. Diaz, V. Petrov, U. Griebner, *Opt. Lett.* **2008**, *33*, 729.
- [313] K. Kieu, F. W. Wise, *IEEE Photon. Tech. Lett.* **2009**, *21*, 128.
- [314] N. N. Il'ichev, E. D. Obraztsova, S. V. Garnov, S. Mosaleva, *Quantum Electron.* **2004**, *34*, 572.
- [315] N. N. Il'ichev, E. D. Obraztsova, P. P. Pashinin, V. I. Konov, S. V. Garnov, *Quantum Electron.* **2004**, *34*, 785.
- [316] A. Martinez, K. Zhou, I. Bennion, S. Yamashita, *Opt. Express* **2008**, *16*, 15425.
- [317] J. W. Nicholson, R. S. Windeler, D. J. DiGiovanni, *Opt. Express* **2007**, *15*, 9176.
- [318] J. C. Jasapara, A. DeSantolo, J. W. Nicholson, A. D. Yablon, Z. Vályay, *Opt. Express* **2008**, *16*, 18869.
- [319] S. Yamashita, Y. Inoue, K. Hsu, T. Kotake, H. Yaguchi, D. Tanaka, M. Jablonski, S. Y. Set, *IEEE Photon. Tech. Lett.* **2005**, *17*, 750.
- [320] K. Kashiwagi, S. Yamashita, S. Y. Set, *Opt. Express* **2008**, *16*, 2528.
- [321] Y. W. Song, S. Y. Set, S. Yamashita, C. S. Goh, T. Kotake, *IEEE Photon. Tech. Lett.* **2005**, *17*, 1623.
- [322] Y.-W. Song, S. Yamashita, C. S. Goh, S. Y. Set, *Opt. Lett.* **2007**, *32*, 148.
- [323] Y.-W. Song, S. Yamashita, E. Einarsson, S. Maruyama, *Opt. Lett.* **2007**, *32*, 1399.
- [324] Y.-W. Song, S. Yamashita, S. Maruyama, *Appl. Phys. Lett.* **2008**, *92*, 021115.
- [325] S. Yamashita, Y. Inoue, S. Maruyama, Y. Murakami, H. Yaguchi, T. Kotake, S. Y. Set, *Jpn. J. Appl. Phys. Part 2* **2006**, *45*, L17.
- [326] N. Nishizawa, Y. Seno, K. Sumimura, Y. Sakakibara, E. Itoga, H. Kataura, K. Itoh, *Opt. Express* **2008**, *16*, 9429.
- [327] K. Kieu, M. Mansuripur, *Opt. Lett.* **2008**, *33*, 64.
- [328] C. A. Poland, R. Duffin, I. Kinloch, A. Maynard, W. A. H. Wallace, A. Seaton, V. Stone, S. Brown, W. MacNee, K. Donaldson, *Nat. Nanotechnol.* **2008**, *3*, 423.
- [329] J. H. Yim, W. B. Cho, S. Lee, Y. H. Ahn, K. Kim, H. Lim, G. Steinmeyer, V. Petrov, U. Griebner, F. Rotermund, *Appl. Phys. Lett.* **2008**, *93*, 161106.
- [330] O. Okhotnikov, T. Jouhti, J. Konttinen, S. Karirinne, M. Pessa, *Opt. Lett.* **2003**, *28*, 364.

- [331] O. G. Okhotnikov, L. Gomes, N. Xiang, T. Jouhti, A. B. Grudinin, *Opt. Lett.* **2003**, *28*, 1522.
- [332] M. E. Fermann, A. Galvanauskas, G. Sucha, D. Harter, *Appl. Phys. B* **1997**, *65*, 259.
- [333] M. E. Fermann, I. Hartl, *IEEE J. Sel. Top. Quantum Electron.* **2009**, *15*, 191.
- [334] M. E. Fermann, M. J. Andrejco, M. L. Stock, Y. Silberberg, A. M. Weiner, *Appl. Phys. Lett.* **1993**, *62*, 910.
- [335] *Ultrafast Lasers, Technology and Applications, Vol. 65* (Eds. M. E. Fermann, A. Galvanauskas, G. Sucha), Marcel Dekker Inc, New York **1997**.
- [336] K. Tamura, L. E. Nelson, H. A. Haus, E. P. Ippen, *Appl. Phys. Lett.* **1993**, *64*, 149.
- [337] L. E. Nelson, D. J. Jones, K. Tamura, H. A. Haus, E. P. Ippen, *Appl. Phys. B* **1997**, *65*, 277.
- [338] K. Tamura, E. P. Ippen, H. A. Haus, L. E. Nelson, *Opt. Lett.* **1993**, *18*, 1080.
- [339] H. A. Haus, K. Tamura, L. E. Nelson, E. P. Ippen, *IEEE J. Quantum Electron.* **1995**, *31*, 591.
- [340] S. M. J. Kelly, *Electron. Lett.* **1992**, *28*, 806.
- [341] F. X. Kartner, U. Keller, *Opt. Lett.* **1995**, *20*, 16.
- [342] F. X. Kartner, I. D. Jung, U. Keller, *IEEE J. Sel. Top. Quantum Electron.* **1996**, *2*, 540.
- [343] D. Y. Tang, S. Fleming, W. S. Man, H. Y. Tam, M. S. Demokan, *J. Opt. Soc. Am. B* **2001**, *18*, 1443.
- [344] K. Tamura, C. R. Doerr, H. A. Haus, E. P. Ippen, *IEEE Photon. Tech. Lett.* **1994**, *6*, 697.
- [345] C. Spielmann, P. F. Curley, T. Brabec, F. Krausz, *IEEE J. Quantum Electron.* **1994**, *30*, 1100.
- [346] G. P. Agrawal, *Lightwave Technology: Telecom. Systems*, Wiley, Hoboken, NJ **2005**.
- [347] D. Von der Linde, *Appl. Phys. B* **1986**, *39*, 201.
- [348] E. A. Avrutin, J. H. Marsh, E. L. Portnoi, *IEE Proc. Optoelectron.* **2000**, *147*, 251.
- [349] K. S. Novoselov, A. K. Geim, S. V. Morozov, D. Jiang, Y. Zhang, S. V. Dubonos, I. V. Grigorieva, A. A. Firsov, *Science* **2004**, *306*, 666.
- [350] A. K. Geim, K. S. Novoselov, *Nat. Mater.* **2007**, *6*, 183.
- [351] A. L. Castro Neto, F. Guinea, N. M. R. Peres, K. S. Novoselov, A. K. Geim, *Rev. Mod. Phys.* **2009**, *81*, 109.
- [352] J. C. Charlier, P. C. Eklund, J. Zhu, A. C. Ferrari, *Top. Appl. Phys.* **2008**, *111*, 673.
- [353] F. Cervantes-Sodi, G. Csanyi, S. Piscanec, A. C. Ferrari, *Phys. Rev. B* **2008**, *77*, 165427.
- [354] S. Novoselov, A. K. Geim, S. V. Morozov, D. Jiang, M. I. Katsnelson, I. V. Grigorieva, S. V. Dubonos, A. A. Firsov, *Nature* **2005**, *438*, 197.
- [355] Y. Zhang, Y. W. Tan, H. L. Stormer, P. Kim, *Nature* **2005**, *438*, 201.
- [356] K. S. Novoselov, Z. Jiang, Y. Zhang, S. V. Morozov, H. L. Stormer, U. Zeitler, J. C. Maan, G. S. Boebinger, P. Kim, A. K. Geim, *Science* **2007**, *315*, 1379.
- [357] S. V. Morozov, K. S. Novoselov, M. I. Katsnelson, F. Schedin, D. C. Elias, J. A. Jaszczak, A. K. Geim, *Phys. Rev. Lett.* **2008**, *100*, 016602.
- [358] X. Du, I. Skachko, A. Barker, E. Y. Andrei, *Nat. Nanotechnol.* **2008**, *3*, 491.
- [359] K. I. Bolotin, K. J. Sikes, Z. Jiang, G. Fundenberg, J. Hone, P. Kim, H. L. Stormer, *Solid State Commun.* **2008**, *146*, 351.
- [360] M. Y. Han, B. Oezylmaz, Y. Zhang, P. Kim, *Phys. Rev. Lett.* **2007**, *98*, 206805.
- [361] Z. Chen, Y. M. Lin, M. Rooks, P. Avouris, *Phys. E* **2007**, *40*, 228.
- [362] Y. Zhang, J. P. Small, W. V. Pontius, P. Kim, *Appl. Phys. Lett.* **2005**, *86*, 073104.
- [363] M. C. Lemme, T. J. Echtermeyer, M. Baus, H. Kurz, *IEEE Electron Device Lett.* **2007**, *28*, 4.
- [364] Y. M. Lin, K. A. Jenkins, A. Valdes-Garcia, J. P. Small, D. B. Farmer, P. Avouris, *Nano Lett.* **2009**, *9*, 422.
- [365] J. S. Bunch, A. M. van der Zande, S. S. Verbridge, I. W. Frank, D. M. Tanenbaum, J. M. Parpia, H. G. Craighead, P. L. McEuen, *Science* **2007**, *315*, 490.
- [366] P. Blake, P. D. Brimicombe, R. R. Nair, T. J. Booth, D. Jiang, F. Schedin, L. A. Ponomarenko, S. V. Morozov, H. F. Gleeson, E. W. Hill, A. K. Geim, K. S. Novoselov, *Nano Lett.* **2008**, *8*, 1704.
- [367] Y. Hernandez, V. Nicolosi, M. Lotya, F. Blighe, Z. Sun, S. De, I. T. McGovern, B. Holland, M. Byrne, Y. Gunko, J. Boland, P. Niraj, G. Duesberg, S. Krishnamurti, R. Goodhue, J. Hutchison, V. Scardaci, A. C. Ferrari, J. N. Coleman, *Nat. Nanotechnol.* **2008**, *3*, 563.
- [368] G. Eda, G. Fanchini, M. Chhowalla, *Nat. Nanotechnol.* **2008**, *3*, 270.
- [369] R. R. Nair, P. Blake, A. N. Grigorenko, K. S. Novoselov, T. J. Booth, T. Stauber, N. M. R. Peres, A. K. Geim, *Science* **2008**, *320*, 1308.
- [370] C. Casiraghi, A. Hartschuh, E. Lidorikis, H. Qian, H. Harutyunyan, T. Gokus, K. S. Novoselov, A. C. Ferrari, *Nano Lett.* **2007**, *7*, 2711.
- [371] E. Lidorikis, A. C. Ferrari, *ACS Nano* **2009**, *3*, 1238.
- [372] D. Sun, Z.-K. Wu, C. Divin, X. Li, C. Berger, W. A. de Heer, P. N. First, T. B. Norris, *Phys. Rev. Lett.* **2008**, *101*, 157402.
- [373] R. W. Newson, J. Dean, B. Schmidt, H. M. van Driel, *Opt. Express* **2009**, *17*, 2326.
- [374] M. Breusing, C. Ropers, T. Elsaesser, *Phys. Rev. Lett.* **2009**, *102*, 4.
- [375] T. Kampfrath, L. Perfetti, F. Schapper, C. Frischkorn, M. Wolf, *Phys. Rev. Lett.* **2005**, *95*, 4.
- [376] J. M. Dawlaty, S. Shivaraman, M. Chandrashekar, F. Rana, M. G. Spencer, *Appl. Phys. Lett.* **2008**, *92*, 042116.
- [377] D. S. L. Abergel, V. I. Fal'ko, *Phys. Rev. B* **2007**, *75*, 155430.
- [378] F. Wang, F. Bonaccorso, D. M. Basko, A. C. Ferrari, **2009**, arXiv: 0909.0457v1.
- [379] M. Hersam, *Nat. Nanotechnol.* **2008**, *3*, 387.
- [380] K. Yanagi, Y. Miyata, H. Kataura, *Appl. Phys. Express* **2008**, *1*, 034003.
- [381] S. N. Kim, Z. Luo, F. Papadimitrakopoulos, *Nano Lett.* **2005**, *5*, 2500.
- [382] H. Ajiki, T. Ando, *Phys. B* **1994**, *201*, 349.
- [383] M. Ichida, S. Mizuno, H. Kataura, Y. Achiba, A. Nakamura, *Appl. Phys. A* **2004**, *78*, 1117.
- [384] Y. Guo, N. Minami, S. Kazaoui, J. Peng, M. Yoshida, T. Miyashita, *Phys. B* **2002**, *323*, 235.
- [385] H. Shimoda, S. J. Oh, H. Z. Geng, R. J. Walker, X. B. Zhang, L. E. McNeil, O. Zhou, *Adv. Mater.* **2002**, *14*, 899.
- [386] Y. Kim, N. Minami, W. H. Zhu, S. Kazaoui, R. Azumi, M. Matsumoto, *J. Appl. Phys.* **2003**, *42*, 7629.
- [387] J. F. Philipps, T. Topfer, H. Eberdorff-Heidepriem, D. Ehrh, R. Saverbrey, N. F. Borelli, *Appl. Phys. B* **2001**, *72*, 175.
- [388] T. Okuno, M. Ikezawa, Y. Masumoto, G. R. Hayes, B. Deveaud, A. A. Lipovskii, *Jpn. J. Appl. Phys. Part 2* **2003**, *42*, L123.
- [389] R. Arenal, A. C. Ferrari, S. Reich, L. Wirtz, J. Y. Mevellec, S. Lefrant, A. Rubio, A. Loiseau, *Nano Lett.* **2006**, *6*, 1812.